

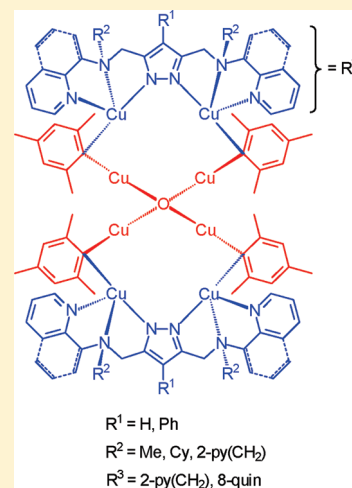
From Pyrazolate-Based Binuclear Copper(I) Complexes to Octanuclear σ -Mesityl-Bridged μ_4 -Oxo-Cuprocuprates: Controlled Dioxygen Splitting by Organocopper Scaffolds

Michael Stollenz,^{*,†} Henrike Gehring, Vera Konstanzer, Stefan Fischer, Sebastian Dechert, Christian Grosse, and Franc Meyer^{*}

Institut für Anorganische Chemie, Georg-August-Universität Göttingen, Tammannstrasse 4, D-37077 Göttingen, Germany

S Supporting Information

ABSTRACT: The synthesis of a series of new pyrazole-based binucleating compartmental ligands, 3,5-bis(R^2R^3N)-(4- R^1)-pyrazoles L^1H-L^6H (L^1H , $R^1 = H$, $R^2 = Me$, $R^3 = 2$ -py(CH_2); L^2H , $R^1 = Ph$, $R^2 = Me$, $R^3 = 2$ -py(CH_2); L^3H , $R^1 = H$, $R^2 = Cy$, $R^3 = 2$ -py(CH_2); L^4H , $R^1 = Ph$, $R^2 = Cy$, $R^3 = 2$ -py(CH_2); L^5H , $R^1 = Ph$, $R^2, R^3 = 2$ -py(CH_2), L^6H , $R^1 = Ph$, $R^2 = Me$, $R^3 = 8$ -quin), together with the X-ray crystal structure of L^3H is reported. After deprotonation and subsequent reaction with 2 equiv of $[Cu^I(CH_3CN)_4](BF_4)$ and PMe_3 , L^3H forms the stable binuclear Cu^I complex $[L^3\{Cu(PMe_3)_2\}_2](BF_4)$ (**1**). The analogous reaction with L^6H and 2 equiv of *tert*-butyl isonitrile affords $[L^6\{Cu(CNtBu)\}_2](BF_4)$ (**2**). **1** and **2** represent the first examples of binuclear Cu^I -pyrazolate complexes of the type $[LCu^I_2]X$ that have been characterized by their X-ray crystal structures. With respect to the planes spanned by the pyrazolate backbone, **1** shows a cis orientation of the PMe_3 ligands, whereas **2** exhibits a trans arrangement of the *t*BuNC ligands. L^1H-L^6H are shown to react with 4 equiv of mesitylcopper and stoichiometric amounts of dioxygen, leading to the formation of the unusually stable organocopper frameworks **3–8**. These complexes follow a general structural principle that is best described by the heteroleptic O-centered cuprate anion $[(MesCu^I)_4(\mu_4-O)]^{2-}$ linked via four trans-oriented σ -mesityl bridges to two flanking binuclear Cu^I -pyrazolates $[(L^1-L^6)Cu^I_2]^+$. Thus, **1** and **2** can also be viewed as capping binuclear Cu^I -complex units that are concealed by two ancillary PMe_3 and *t*BuNC ligands, respectively. The exemplary reaction of **4** with an excess of dimethyl acetylenedicarboxylate (DMDAC) supports the observed cuprate features of **3–8**, since after hydrolysis the corresponding (syn-)addition product $MesC(CO_2Me)=C(CO_2Me)H$ (**9**) and the free ligand L^2H are found as major products.



INTRODUCTION

Organocopper chemistry has attracted considerable interest over the last few decades, which is attributed to its high and versatile potential in synthetic chemistry.¹ This is, for instance, reflected by the unique role of copper in the activation of dioxygen, as demonstrated by important transformations such as the catalytic oxidation of ethylene to ethylene glycol, the Wacker process, and the oxidative coupling of acetylenes and of biaryls.^{2–4} Another large area of importance is represented by organocuprates and their stoichiometric and catalytic applications as selective transfer reagents that generate valuable organic building blocks.^{1,5}

Although organocopper reagents provide this broad range of useful synthetic methodologies, relatively little is known about the specific role of such species in oxidatively induced C–C coupling reactions and cuprate-type transformations. To elucidate the structural role of organocuprates in the latter types of reactions, valuable approaches were made by employing mesitylcopper⁶ as a well-defined and well-characterized precursor. Its use is convenient for the synthesis of a variety of unusual yet relatively stable organocopper frameworks which serve as potential

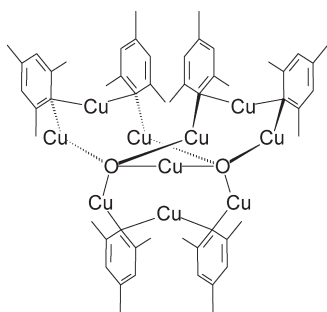
intermediates in cuprate-involving reactions. This has been demonstrated earlier for the unique cuprocuprate $[(DPPE)_2Cu][CuMes_2]$ (DPPE = 1,2-bis(diphenylphosphino)ethane) by Leoni, Pasquali, and Ghilardi,⁷ and later for magnesium organocuprates bearing arenethiolate coligands by van Koten et al.,^{1,8} and recently again for several intriguing lithium and magnesium organocuprates by Davies et al.⁹ A real breakthrough en route to a deeper insight into oxidative copper-mediated C–C couplings was also achieved with mesitylcopper, namely its controlled oxygenation resulting in the formation of bimesityl and the unusual complex array $[Cu_{10}O_2Mes_6]$ (Chart 1).¹⁰ According to an X-ray structure determination, this remarkable compound consists of ten Cu^I centers which are held together by two μ_4 -O bridges and six μ - σ -mesityl linkers. Further spectroscopic investigations of this highly sensitive framework still remain a challenging goal and have not been reported so far.

We have recently communicated an exceptionally stable octanuclear σ -mesitylcopper complex with a related structure

Received: August 27, 2010

Published: April 13, 2011

Chart 1. Cu^{I} Complex Framework Obtained from Mesityl-copper and Dioxygen

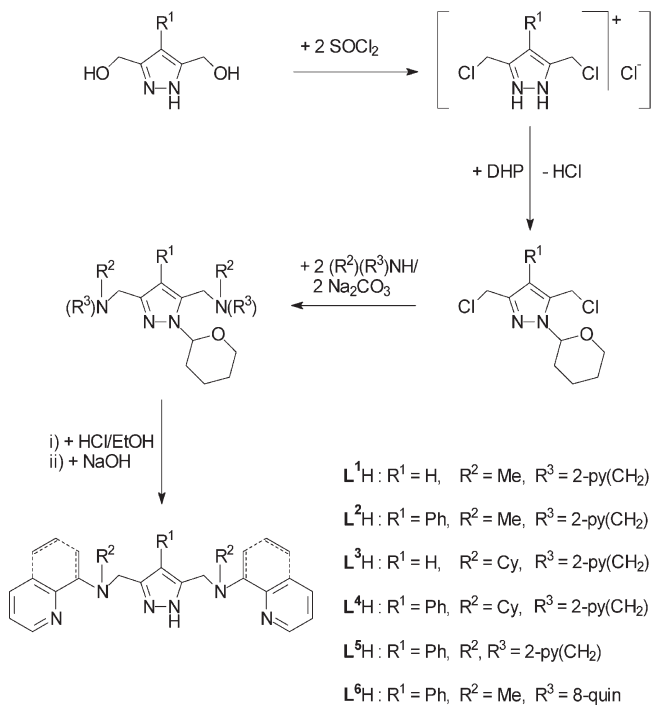


consisting of a complex cuprate anion, $[(\text{MesCu}^{\text{I}})_4(\mu_4\text{-O})]^{2-}$, that is encapsulated by two flanking, and thus stabilizing, binuclear Cu^{I} -pyrazolates $[(\text{L}^2)\text{Cu}^{\text{I}}_2]^+$; it was obtained from the reaction of two chelating ligands, 8 equiv of mesitylcopper, and $1/2$ equiv of dioxygen.¹¹ Multinuclear pyrazolate-based compartmental ligands have attracted considerable interest over the course of the past decade, since they allow the positioning of two metal centers in close proximity, thus resulting in bi- or oligomeric frameworks with unique structural features and synergistic electronic or magnetic properties, using Cu^{II} and other metals.^{2b,12,13} Fine-tuning of the bimetallic arrangement is achieved by combining the negatively charged pyrazolate backbone, which acts as the bridging core of the ligand system to hold two metal centers at a distance of around 3.0–4.5 Å to each other, with suitable appended donor side groups at the 3,5-positions of the central heterocyclic ring providing variable binding pockets. Since mesitylcopper is known to form tetrameric or pentameric cyclic arrays $[\text{CuMes}]_n$ in the solid state with interatomic distances between next but one neighboring Cu atoms in the range of about 3.40–4.15 Å,^{6b-d} we reasoned that pyrazolate-based compartmental ligand systems should offer the right premise to host two terminal Cu^{I} centers of a tailored fragment of mesitylcopper such as $[\text{Cu}(\mu_2\text{-Mes})\text{Cu}(\mu_2\text{-Mes})\text{Cu}]^+$ or $[\text{Cu}(\mu_2\text{-Mes})\text{Cu}(\mu_2\text{-Mes})\text{Cu}(\mu_2\text{-Mes})\text{Cu}]^+$; this has indeed been supported by our recent preliminary results.¹¹

In this context we have now been interested in gaining deeper insight into the various structural features of those complex frameworks, in particular those features that are related to their cuprate character and the resulting reactivity in dependence of different stabilizing pyrazolate scaffolds. This requires the initial synthesis of smaller Cu^{I} building blocks of the type $[\text{LCu}_2]^+$, which represent the stabilizing capping units in the previously reported $[(\text{L}^2)\text{Cu}^{\text{I}}_2(\mu_2\text{-MesCu}^{\text{I}})_2(\mu_4\text{-O})(\mu_2\text{-MesCu}^{\text{I}})_2(\text{L}^2)\text{Cu}^{\text{I}}_2]$.

It has also previously been demonstrated that the nuclearity of usually trimeric or tetrameric Cu^{I} and Ag^{I} pyrazolates^{14–16} can be controlled by using ancillary strong σ -donor or π -acceptor ligands such as phosphines, isonitriles, and CO.¹⁷ However, it has remained a great challenge to find appropriate methods for synthesizing binuclear Cu^{I} species with compartmental pyrazolate scaffolds that are structurally related to the established binuclear Cu^{II} pyrazolate complexes. Prerequisite for the targeted preparation of binuclear Cu^{I} pyrazolate species is a well-adjusted combination of the donor/acceptor strengths of the coligands and the presence of two suitable binding pockets at the central pyrazolate bridging unit. Otherwise, alternative binding modes and nuclearities are obviously favored over the desired binuclear arrangement (vide infra).

Scheme 1. Synthesis of $\text{L}^{\text{I}}\text{H}-\text{L}^{\text{6}}\text{H}$



Herein, we describe the synthesis of four new compartmental pyrazole ligands and the first X-ray crystal structure determination of a pyrazole derivative with $\{\text{N}_2\}$ ligating chelate arms at the 3,5-positions of the heteroaromatic core. Second, the synthesis and structural characterization of the first two examples of binuclear Cu^{I} pyrazolate complexes of the type $[\text{L}(\text{Cu}^{\text{I}})_2]\text{X}$ are reported. Finally, we report on a series of unusual organocopper oligomeric frameworks of the general composition $[(\text{L}^{\text{I}}-\text{L}^{\text{6}})\text{Cu}_2(\mu_2\text{-MesCu}^{\text{I}})_2(\mu_4\text{-O})(\mu_2\text{-MesCu}^{\text{I}})_2(\text{L}^{\text{I}}-\text{L}^{\text{6}})\text{Cu}_2]$, which bear close structural relation to the binuclear complexes; we describe their spectroscopic properties together with some remarkable structural features, and we also give an example for the reactivity of those organocopper assemblies toward activated alkynes.

RESULTS AND DISCUSSION

Synthesis of the Ligands and X-ray Crystal Structure Determination of $\text{L}^{\text{3}}\text{H}$. The new ligands $\text{L}^{\text{1}}\text{H}$ and $\text{L}^{\text{3}}\text{H}-\text{L}^{\text{5}}\text{H}$ are accessible by a proven multistep synthetic sequence that was described earlier for $\text{L}^{\text{2}}\text{H}$ and $\text{L}^{\text{6}}\text{H}$ (Scheme 1).^{11,15} They all can be readily prepared from the starting materials 3,5-bis(hydroxymethyl)-1H-pyrazole¹⁸ and 3,5-bis(hydroxymethyl)-4-phenyl-1H-pyrazole¹⁹ and the respective secondary amines; the products are isolated as viscous oils ($\text{L}^{\text{1}}\text{H}$ and $\text{L}^{\text{5}}\text{H}$) or powders ($\text{L}^{\text{3}}\text{H}$ and $\text{L}^{\text{4}}\text{H}$) in reasonable to good overall yields (37–85%).

$\text{L}^{\text{1}}\text{H}$ is readily soluble in polar solvents such as THF and acetonitrile as well as in CH_2Cl_2 and CDCl_3 , whereas its solubility in benzene or toluene is rather low. All other new ligands bearing nonpolar side groups such as phenyl and cyclohexyl can be dissolved also in the less polar solvents without restrictions. The HR-ESI(+) spectra of all four new ligands $\text{L}^{\text{1}}\text{H}$ and $\text{L}^{\text{3}}\text{H}-\text{L}^{\text{5}}\text{H}$ exhibit the expected $[\text{M} + \text{H}]^+$ peaks, which are in good agreement with their calculated isotopic distribution patterns (see Experimental Section). Slow evaporation of a saturated

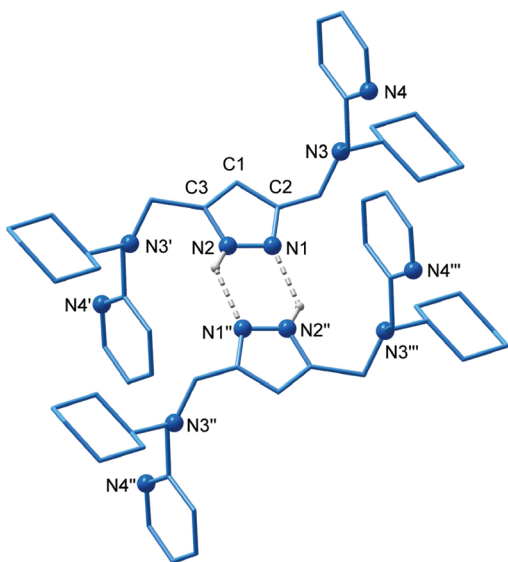


Figure 1. Representation of two hydrogen-bridged molecules of L^3H . Hydrogen atoms, except those forming hydrogen bridges, have been omitted for clarity. Selected interatomic distances (Å) and bond angles (deg): $N1-N2 = 1.3449(16)$, $N1-C2 = 1.319(2)$, $N2-C3 = 1.362(3)$, $C1-C2 = 1.401(2)$, $C1-C3 = 1.379(2)$, $N2 \cdots N1'' = 2.8994(17)$; $N1-N2-C3 = 113.52(13)$, $N2-N1-C2 = 104.90(13)$. Symmetry operations used to generate equivalent atoms: (') $1-x, 1-y, 1-z$; (') $1-x, -y, 1-z$; (') $x, -1+y, z$.

solution of L^3H in diethyl ether at room temperature afforded colorless crystals suitable for an X-ray crystal structure determination. L^3H crystallizes in the monoclinic space group $P2_1/c$. Its molecular structure is shown in Figure 1, together with selected bond distances and angles.

The solid-state structure of L^3H confirms the expected symmetrical arrangement of the side arms at the 3,5-positions of the pyrazole backbone. As reported earlier for only a few pyrazoles,²⁰ in the crystal lattice of L^3H two molecules are arranged in $NH \cdots N$ bridged dimeric pairs, as indicated by close intermolecular donor–acceptor distances between the pyrazole N atoms ($N2 \cdots N1'' = 2.8994(17)$ Å). However, since the pyrazole units in L^3H are disordered, these distances should be considered with care. The planes spanned by each of the two pyrazole heterocyclic rings connected by hydrogen bridges are almost parallel but not coplanar, as shown by their distance of approximately 0.28 Å. This dimeric arrangement is rarely observed, since generally more common structural motifs for pyrazoles forming N–hydrogen bridges are cyclic trimers, tetramers, or catemers.^{20a,21}

Both the 1H and ^{13}C NMR spectra of L^1H , monitored in $CDCl_3$ at room temperature, display only one set of signals attributed to the $-CH_2N(CH_3)(2\text{-pyridyl})$ side arms, thus suggesting fast rotation around the C–C and C–N bonds of these groups as well as a fast proton exchange due to the pyrazole N–H tautomerism. A characteristic singlet at δ 6.16 ppm (^{13}C 105.1 ppm) reflects the 4-pyrazole proton (CH) of L^1H ; the corresponding resonances of L^3H appear at δ 6.33 and 103.2 ppm in the 1H and ^{13}C NMR spectra recorded in benzene- d_6 . Also in the case of L^3H and L^4H only one set of signals related to the considerably bulkier $-CH_2N(Cy)(2\text{-pyridyl})$ side groups is observed. However, line broadening of the signals of the hinge CH_2 groups and of the $\alpha\text{-CH}^{Cy}$ proton signal increases from

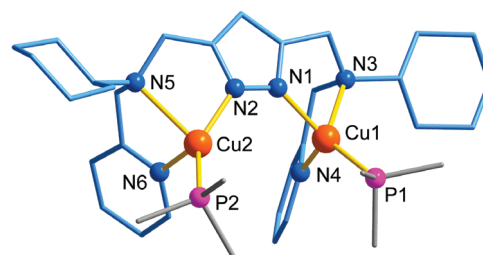


Figure 2. Molecular structure of the complex cation of one (A) of the two independent molecules of **1**. The BF_4^- counterion and hydrogen atoms have been omitted for clarity. Selected interatomic distances (Å) and bond angles (deg): $N1-N2 = 1.355(4)$, $Cu1-P1 = 2.1499(11)$, $Cu1-N1 = 1.983(3)$, $Cu1-N3 = 2.249(3)$, $Cu1-N4 = 2.067(3)$, $Cu2-P2 = 2.1771(12)$, $Cu2-N2 = 1.981(3)$, $Cu2-N5 = 2.394(3)$, $Cu2-N6 = 2.094(3)$, $Cu1 \cdots Cu2 = 4.2778(16)$; $P1-Cu1-N1 = 126.11(8)$, $P1-Cu1-N3 = 127.51(8)$, $P1-Cu1-N4 = 119.72(9)$, $N1-Cu1-N3 = 80.87(10)$, $N1-Cu1-N4 = 108.28(12)$, $N3-Cu1-N4 = 80.94(11)$, $P2-Cu2-N2 = 143.69(9)$, $P2-Cu2-N5 = 124.54(7)$, $P2-Cu2-N6 = 110.58(8)$, $N2-Cu2-N5 = 77.31(11)$, $N2-Cu2-N6 = 101.53(11)$, $N5-Cu2-N6 = 78.70(10)$.

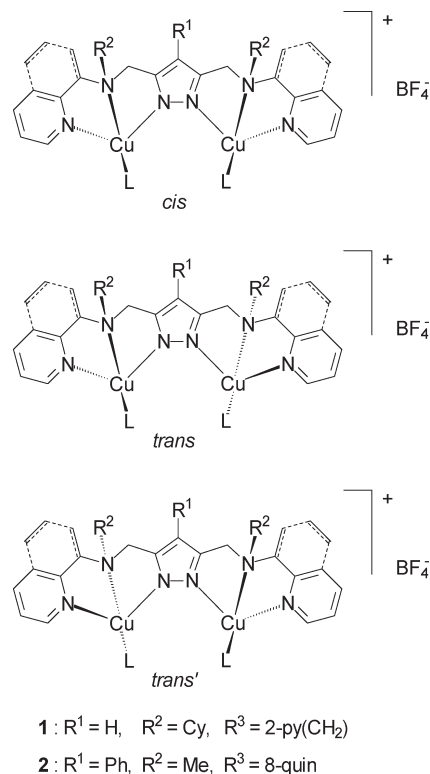
L^3H to L^4H , indicating a limited free rotation of the cyclohexyl, pyridyl, and even phenyl substituents around their C–C and C–N bonds. Again, this effect of steric hindrance occurs in the 1H NMR spectrum of L^5H (benzene- d_6 at room temperature), whose CH_2 resonance is clearly broadened, whereas the aromatic signals are sharp and display four pyridyl groups that appear to be equivalent in solution.

Synthesis, Properties, and X-ray Crystal Structure Determinations of Complexes 1 and 2. Dicopper(I) complexes could be isolated and structurally characterized in two cases. Deprotonation of L^3H or L^6H with a strong base ($NaN(SiMe_3)_2$ or $KOtBu$) and subsequent reaction with 2 equiv of $[Cu^I(CH_3CN)_4](BF_4)$ and 2 equiv of a coligand (PMe_3 or $tBuNC$) afforded the complexes $[L^3\{Cu(PMe_3)\}_2]BF_4$ (**1**) and $[L^6\{Cu(CNtBu)\}_2]BF_4$ (**2**) as pale yellow and beige solids, respectively. Elemental analyses and characteristic fragments of the ESI(+) mass spectra confirm the proposed compositions (see the Experimental Section for details).

1 is readily soluble in THF and reasonably in toluene, but only sparingly in diethyl ether. Both in solution and in the solid state this complex is moderately air stable, but it can be stored under an atmosphere of argon for a longer time period. Decomposition takes place in air, presumably by releasing PMe_3 , thus resulting in a green compound, which is very likely a Cu^{II} species. The solubility of **2** is more restricted to polar solvents such as CH_2Cl_2 , THF, and acetonitrile, since the complex is poorly soluble in toluene. **2** is also moderately air stable and can be stored under inert conditions for several months.

Single crystals of **1** suitable for an X-ray crystal structure determination were grown by slow diffusion of diethyl ether into a THF solution at $+4$ °C. **1** crystallizes in the triclinic space group $P\bar{1}$ with two independent molecules in the asymmetric unit and two disordered BF_4^- counterions (see the Supporting Information). The molecular structure of one complex cation (A), whose bond distances and angles of the chelating backbone only slightly differ from those of the second cation (B), is depicted in Figure 2.

As anticipated from the analytical results, the X-ray molecular structure of **1** shows a binuclear, cationic copper(I) pyrazolate complex with distorted-tetrahedral coordination of the two metal centers, each bearing one ancillary PMe_3 as a coligand.

Chart 2. Isomers of **1** and **2**

The BF_4^- counterion is found to be separated from the cationic complex unit. The distortion of both Cu^{I} centers is reflected by the angles $\text{P}-\text{Cu}-\text{N}$ and $\text{N}-\text{Cu}-\text{N}'$, which range from $77.31(11)$ to $143.69(9)^\circ$ and clearly deviate from an ideal tetrahedral angle. The $\text{Cu}-\text{P}$ bonds are slightly different ($2.1499(11)$ and $2.1771(12)$ Å) but lie in the range observed for other $\text{Cu}^{\text{I}}(\text{PMe}_3)$ complexes involving chelating ligands.^{22,23} Due to the anionic character of the pyrazolate bridge, the $\text{Cu}-\text{N}^{\text{Pz}}$ bonding distances are significantly shorter ($1.981(3)$ and $1.983(3)$ Å) than those between the copper ions and the pyridyl donor atoms ($2.067(3)$ and $2.094(3)$ Å). As expected, the aliphatic $(\text{Cy})\text{N}(\text{CH}_2)$ hinges that lack any back-bonding capability show even longer $\text{Cu}-\text{N}$ distances ($2.249(3)$ and $2.394(3)$ Å). If only the three stronger donor atoms of each binding pocket are considered, coordination of the Cu^{I} ions can be described as almost trigonal, as revealed by the sums of the corresponding binding angles at $\text{Cu}1$ ($354.11(12)^\circ$) and $\text{Cu}2$ ($355.80(11)^\circ$). These values are much closer to the sum of the binding angles expected for an ideal trigonal-planar coordination geometry (360°) than the sum of three angles of an ideal tetrahedron (328.5°). Another Cu^{I} complex with a related multinuclear scaffold and ancillary PMe_3 ligands was recently reported by our group.²³ This complex of the composition $[\text{L}_2\text{Cu}_4(\text{PMe}_3)_2](\text{PF}_6)$ ($\text{L} = (\text{Me-imidazolyl})_2(\text{C}-\text{OMe})(3,5\text{-pz})(\text{C}-\text{OMe})(\text{Me-imidazolyl})_2$) indeed bears four Cu^{I} centers with distorted-trigonal coordination arranged in a more complicated fashion than in **1**, however, with very similar $\text{Cu}-\text{P}$ and $\text{Cu}-\text{N}^{\text{Pz}}$ bonding distances. This confirms the general tendency of Cu^{I} to form complexes with coordination numbers lower than 4, especially in these types of multinuclear complexes based on compartmental pyrazolate scaffolds, which overall behave as comparatively strong donors toward the embedded metal centers.

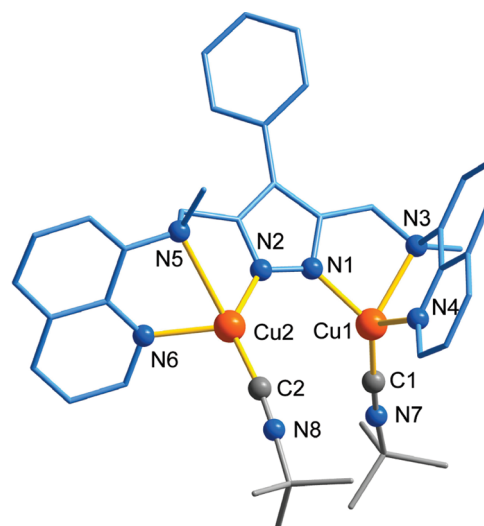


Figure 3. Molecular structure of the complex cation of **2**. The BF_4^- counterion and hydrogen atoms have been omitted for clarity. Selected interatomic distances (Å) and bond angles (deg): $\text{N}1-\text{N}2 = 1.368(4)$, $\text{Cu}1-\text{C}1 = 1.827(4)$, $\text{Cu}1-\text{N}1 = 2.014(2)$, $\text{Cu}1-\text{N}3 = 2.232(3)$, $\text{Cu}1-\text{N}4 = 2.042(3)$, $\text{Cu}2-\text{C}2 = 1.867(3)$, $\text{Cu}2-\text{N}2 = 1.949(3)$, $\text{Cu}2-\text{N}5 = 2.691(3)$, $\text{Cu}2-\text{N}6 = 2.093(3)$, $\text{Cu}1 \cdots \text{Cu}2 = 4.0552(6)$; $\text{C}1-\text{Cu}1-\text{N}1 = 130.74(13)$, $\text{C}1-\text{Cu}1-\text{N}3 = 119.95(13)$, $\text{C}1-\text{Cu}1-\text{N}4 = 125.42(12)$, $\text{N}1-\text{Cu}1-\text{N}3 = 79.49(10)$, $\text{N}1-\text{Cu}1-\text{N}4 = 100.83(10)$, $\text{N}3-\text{Cu}1-\text{N}4 = 81.04(10)$, $\text{C}2-\text{Cu}2-\text{N}2 = 132.72(13)$, $\text{C}2-\text{Cu}2-\text{N}5 = 137.99(13)$, $\text{C}2-\text{Cu}2-\text{N}6 = 108.08(13)$, $\text{N}2-\text{Cu}2-\text{N}5 = 74.97(9)$, $\text{N}2-\text{Cu}2-\text{N}6 = 116.78(10)$, $\text{N}5-\text{Cu}2-\text{N}6 = 69.35(9)$.

With respect to the plane spanned by the pyrazolate backbone, the two PMe_3 ligands in **1** are oriented to the same side of this plane with distances $\text{P}1 \cdots \text{Pz} = 1.052(1)$ Å and $\text{P}2 \cdots \text{Pz} = 0.467(1)$ Å (Pz = plane of the pyrazolate ring).²⁴ This is best described as a cis arrangement of the ancillary phosphine ligands and, at the opposite side of the Pz plane, also of the chelating pyridyl side groups (Figure S3, Supporting Information).²⁵

^1H NMR spectra of **1** (recorded in benzene- d_6 as well as in THF- d_8) show one set of signals related to the chelating $-\text{CH}_2\text{N}-$ (Cy)(2-pyridyl) side groups, as observed also for the free ligand L^3H . One additional sharp doublet at δ 1.27 ppm ($^2J_{\text{HP}} = 5.9$ Hz) in the benzene- d_6 spectrum and at δ 1.28 ppm ($^2J_{\text{HP}} = 5.8$ Hz) in the spectrum recorded in THF- d_8 shows the presence of two equivalent PMe_3 ligands, which suggests that the 2-fold symmetry of the molecular structure of **1** found in the solid state is retained in solution. Comparison of the ^1H NMR benzene- d_6 spectra of L^3H and **1** reveals considerable downfield shifts of the signals assigned to the 5- and 6-pyridyl protons by about 0.89 and 0.74 ppm, which can be attributed to the two coordinated Cu^{I} centers. The 3-pyridyl protons and the 4-pyrazolate proton are shifted to higher field by around 0.98 and 0.33 ppm, whereas the resonance signals related to the 4-pyridyl proton and the aliphatic cyclohexyl protons show no substantial changes. The proton signals of the hinge CH_2 groups are clearly shifted and become somewhat broadened. A similar trend of chemical shift changes between L^3H and **1** is also observed in the corresponding ^{13}C NMR spectra (see the Experimental Section). When a solution of **1** in benzene- d_6 is stored at room temperature for longer times, in the ^1H NMR spectrum a remarkable high-field shift of the 6-pyridyl proton signal of 0.14 ppm and downfield shifts of the 3- and 4-pyridyl proton signals of 0.17 and 0.14 ppm are observed, while the remaining resonance signals show no

significant alterations. Since these aromatic protons may be strongly affected by conformational and electronic changes at the coordination spheres of the two Cu^{I} ions, we believe that a slow isomerization process of **1** occurs in solution, presumably from the *cis* to the *trans* isomer (Chart 2). This interpretation is supported by the solid-state structure of the related complex **2**, which indeed shows a *trans* disposition of the ancillary ligands.

Slow diffusion of diethyl ether into a solution of **2** in CH_2Cl_2 at $+4^\circ\text{C}$ afforded light yellow crystals suitable for an X-ray crystal structure determination. **2** was found to crystallize in the triclinic space group $P\bar{1}$ (like complex **1**) with the cationic complex unit, the BF_4^- counterion, and one CH_2Cl_2 molecule in the asymmetric unit. As also observed for **1**, the BF_4^- anion is clearly separated from the cationic complex unit. Figure 3 shows the binuclear complex cation, together with selected interatomic distances and bond angles.

In agreement with the spectroscopic results, the molecular structure of the complex cation of **2** in the solid state displays the expected bimetallic arrangement with one ancillary *t*BuNC ligand per metal ion. Similar to the case for **1**, both Cu^{I} atoms are found in distorted-tetrahedral environments. Again, the sum of the binding angles related to the more strongly binding donor atoms C1, N1, and N4 ($356.99(13)^\circ$ at Cu1) as well as C2, N2, and N6 ($357.58(13)^\circ$ at Cu2) reflects the tendency of both cuprous ions in **2** to prefer a trigonal-planar over a tetrahedral coordination sphere. Interestingly, the aliphatic N donors N3 and N5 of the chelating $-\text{CH}_2\text{N}(\text{Me})(8\text{-quinolyl})$ side groups show very different Cu–N bond lengths. The interatomic separation between N5 and Cu2 of $2.691(3)\text{ \AA}$ is quite large, albeit below the sum of the van der Waals radii of N and Cu of 2.95 \AA .²⁶ In fact, one may expect a relatively weak σ -donor strength of N3 and N5 because of the electron-withdrawing quinolyl rings. In the case of N3, however, a remarkable close bonding distance (Cu1–N3 = $2.232(3)\text{ \AA}$) is observed that is equal or even shorter than the corresponding Cu–N(Cy) bonds in **1**. This is somewhat surprising, since in the solid-state structure of the homoleptic complex $[\text{L}^6\text{Cu}]_4$ ¹⁵ the $\text{Cu}\cdots\text{N}$ distances involving the hinge N(Me) groups are clearly out of the range of any bonding interaction. As the ^1H and ^{13}C NMR spectra (THF- d_8 at room temperature) indicate, complex **2** adopts a highly symmetric structure in solution or is highly fluxional. Therefore, the (Me)N donor functions in the chelating side groups are anticipated to act as hemilabile ligands, and the close Cu1–N3 bonding distance is presumably forced by packing effects as well as particularly by π – π stacking interactions in the crystal structure of **2**. Such stacking mainly involves the peripheral quinolyl groups, as displayed in Figure 4. Similar π – π contacts have been reported recently also for the homoleptic Cu^{I} complex $[\text{L}^6\text{Cu}]_4$, which shows an extended network of π – π stacking in its crystal lattice.¹⁵ This additional driving force seems to dominate the orientation of these weakly coordinating, hemilabile side arm donor groups in the solid state.

Considering the orientation of both *t*BuNC coligands relative to the plane spanned by the pyrazolate backbone, the solid-state molecular structure of **2** represents a *trans* isomer, in contrast to the corresponding *cis* arrangement that is observed in **1** (Figures S3 and S6, Supporting Information).

Thus, in **2** the ancillary *t*BuNC ligands are oriented to opposite sides of the pyrazolate plane. Distortion of the coordination spheres at both copper centers is considerably more pronounced than in **1**, as reflected by the different distances of the isonitrile C ($1.513(4)$ and $0.979(4)\text{ \AA}$) to the plane. Similar differences are

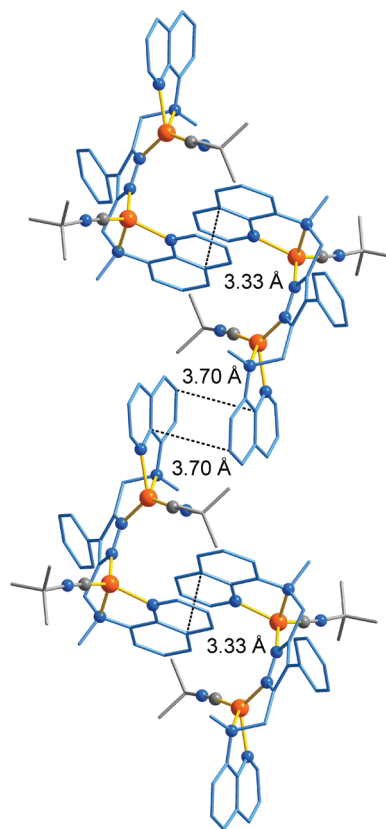


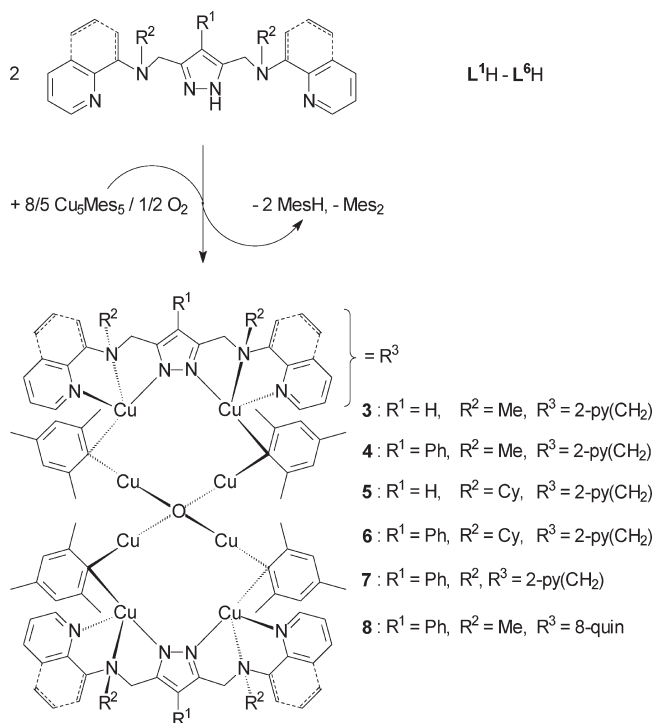
Figure 4. Representation of four complex molecule cations of the crystal structure of **2**. Intermolecular π – π stacking is highlighted by the closest $\text{C}\cdots\text{C}$ distances shown.

observed for the corresponding distances between the N-quinolyl donors and the pyrazolate plane ($1.859(3)$ and $0.593(3)\text{ \AA}$).²⁴ The observed *trans* orientation of the coligands (and of the peripheral donor groups) in **2** supports our assumption that **1** may undergo slow conversion in solution from the *cis* (C_s) to the *trans* (C_2) isomers according to Chart 2. As indicated by the inversion center in space group $P\bar{1}$, both enantiomers of **2** (with its idealized noncrystallographic C_2 symmetry) are present in the crystal lattice. These two enantiomers formally interconvert by changing the positions of the ancillary isonitrile ligands with respect to the chelating quinolyl side arms at *both* copper centers.

As is the case for **1**, the ^1H NMR spectrum of complex **2**, monitored in THF- d_8 at room temperature, shows only one set of signals for the chelating side groups as well as for the phenyl group attached to the pyrazolate heterocycle. Additionally, a slightly broadened singlet at δ 1.56 ppm is assigned to the two *t*BuNC coligands and shows that **2** has 2-fold symmetry on the NMR time scale. Significant shifts of the aromatic proton signals (that also appear as only one set) of **2** in comparison to its free ligand L^6H confirm that both Cu^{I} ions remain coordinated in solution. For example, the quinolyl H^2 protons, which are the closest atoms to the coordinating quinolyl-N donor groups, show a downfield shift of about $+0.45$ ppm. In the ^{13}C NMR spectrum of **2** the corresponding quinolyl C^2 resonance signal is shifted by $+4.3$ ppm.

Synthesis, Properties, and X-ray Crystal Structure Determinations of the Organocopper Complexes 3–8. Compounds **3–8** can be obtained from the reactions of $\text{L}^1\text{H}–\text{L}^6\text{H}$ with mesitylcopper in a molar ratio of 1:4 in THF or toluene

Scheme 2. Synthesis of Complexes 3–8



solutions at -78°C and subsequent treatment with stoichiometric amounts of dioxygen at room temperature; they are isolated as yellow to beige solids in yields of 48–87%. Excess dioxygen results in decomposition, as evidenced by the formation of insoluble brownish solids and mesitylene. The byproducts mesitylene and bimesityl resulting from the stoichiometric reaction, which both strongly support the reaction pathway sketched in Scheme 2, were identified by ^1H NMR (in a 1:2.6 ratio of bimesityl to mesitylene).^{11,27}

Elemental analyses of 3–8 confirm the composition $[(\text{L}^3\text{--L}^6)(\text{Cu}_4\text{Mes}_2\text{O}_{0.5})]$. Their ESI(+) spectra show several representative fragments of oligonuclear organocopper species such as $[\text{LCu}_2\text{Mes} + 1]^+$ for **4**¹¹ or $[\text{LCu}_2\text{Mes}_2\text{Cu}_2]^+$ (**3** and **5–7**) and even $[\text{LCu}_2\text{Mes}_2\text{CuO} + 1]^+$ in the case of **8** (see also the Experimental Section). Complexes 3–8 are sensitive to air and moisture both in solution and in the solid state. However, under argon, they are stable at room temperature for several months. All organocopper compounds are readily soluble in THF, toluene, and C_6D_6 , whereas their solubility in diethyl ether is considerably lower. Complex **6** represents an exception, since this compound bears six large, nonpolar substituents (two phenyl, four cyclohexyl) and is therefore also readily soluble in diethyl ether and even slightly in *n*-pentane.

Single crystals suitable for X-ray crystal structure analyses were grown from THF (**3** and **4**), toluene (**5**, **7**, and **8**) or diethyl ether (**6**) by slow diffusion of diethyl ether (**3–5**, **7**, and **8**) or *n*-pentane (**6**) into the respective solutions at $+4^\circ\text{C}$ (**3**, **4**, and **6–8**) or -18°C (**5**). The result of the structure determination of **5** is depicted in Figure 5; selected atom distances and bond angles of 3–8 are collected in Tables 1 and 2 (for further information about the X-ray molecular structures of **3** and **6** see also the Supporting Information). In the case of complex **3**, two complex molecules—one with disorder in the pyrazolate backbone—were found in the asymmetric unit (see also X-ray

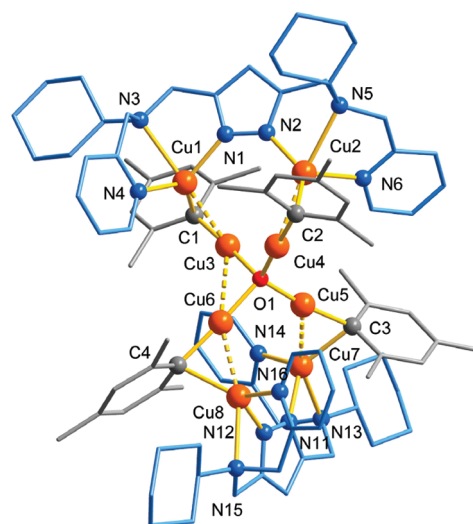


Figure 5. Molecular structure of **5**. Hydrogen atoms have been omitted for clarity. $\text{Cu}\cdots\text{Cu}$ contacts are represented as dashed lines.

Crystallography and the Supporting Information). Similarly, **6** also contains two independent complex molecules in the asymmetric unit of the crystal lattice. Since in both **3** and **6** the complex molecules are similar, only the data of one molecule are discussed herein. The corresponding data for complex **4** were previously communicated.¹¹ Complexes **5** and **6** show disorder for some of the cyclohexyl rings which are not displayed in Figures 5 and Figures S10–S13 (see the Supporting Information), respectively. The X-ray crystal structure determination for **7** reveals disordered noncoordinating pyridyl groups and a disordered phenyl substituent at the pyrazolate scaffold embedding Cu7 and Cu8 as well. This is, however, not shown in Figure 6 (and Figure S15).

At first glance, all organocopper complexes adopt very similar structures. Each of them features a distorted pseudo tetrahedral $(\mu_4\text{-O})\text{Cu}_4$ core with tethered σ -mesityl bridging ligands that are linked to two binuclear Cu^1 -pyrazolato scaffolds in a three-center–two-electron bonding mode; such a bonding situation is well-known from homoleptic σ -organocopper compounds such as $[\text{Cu}_4\text{Mes}_4]$, $[\text{Cu}_5\text{Mes}_5]$, and $[\text{Cu}_4(\text{CH}_2\text{SiMe}_3)_4]$.^{6b–d,28} Overall, 3–8 represent octanuclear organocopper frameworks with two distinct sets of Cu^1 centers that are shielded by two pyrazolate chelating scaffolds. However, in the case of complex **8**, the hemilabile character of ligand L^6 leads to some remarkable structural deviations from this general motif (vide infra).

Peripheral copper ions hosted by the $\{\text{N}_3\}$ binding pockets of the pyrazolate ligands are all found in distorted-tetrahedral environments (except for **8**), even in the presence of additional donor functions such as in complex **7**. Drastic distortion of the tetrahedral coordination sphere may arise not only from the constraints of the binding framework of the chelating ligand but also from contributions by cuprophilic $d^{10}\cdots d^{10}$ contacts with the central metal ions. If one considers such interactions, coordination polyhedra might be best described as pseudo trigonal bipyramidal. This is conclusive by τ values ranging from 0.52 to 0.70 for 3–7, although one (in **4A**) or two (in **5**) coordination polyhedra are slightly closer to the square-pyramidal coordination mode ($\tau = 0.48\text{--}0.50$, Table 3).²⁹

The situation for complex **8** is clearly different, since only three peripheral copper centers show pentacoordination at all. The

Table 1. Selected Bond Lengths (Å) of 3–8

	3A	4A	5	6A	7	8
Cu1–N1	1.981(9)	1.986(5)	2.000(4)	1.9998(15)	1.981(4)	1.928(4)
Cu2–N2	2.009(9)	1.962(6)	1.971(4)	1.9944(15)	1.992(4)	2.003(4)
Cu7–N11	2.026(15)	2.018(5)	1.992(4)	2.0079(14)	2.008(5)	2.021(5)
Cu8–N12	1.972(15)	1.982(6)	1.989(4)	2.0142(14)	1.969(5)	1.892(4)
Cu1–N3	2.412(9)	2.387(5)	2.408(4)	2.4751(15)	2.409(4)	2.589(6)
Cu2–N5	2.322(9)	2.323(5)	2.419(4)	2.4529(16)	2.375(3)	2.401(4)
Cu7–N13	2.374(12)	2.370(5)	2.452(4)	2.4224(14)	2.313(4)	2.381(4)
Cu8–N15	2.368(11)	2.323(5)	2.411(5)	2.4774(15)	2.321(4)	2.711(6)
Cu1–N4	2.045(9)	2.039(5)	2.038(4)	2.0294(15)	2.031(4)	2.454(5)
Cu2–N6	2.069(9)	2.090(6)	2.077(4)	2.1167(16)	2.038(4)	2.096(5)
Cu7–N14	2.121(13)	2.082(6)	2.046(4)	2.0619(14)	2.062(5)	2.048(5)
Cu8–N16	2.084(11)	2.072(5)	2.056(4)	2.1012(15)	2.073(5)	3.034(6)
Cu1–C1	2.141(11)	2.115(7)	2.147(5)	2.1223(19)	2.146(4)	2.047(5)
Cu2–C2	2.137(11)	2.104(7)	2.124(5)	2.1462(18)	2.138(4)	2.131(6)
Cu7–C3	2.171(12)	2.157(7)	2.120(5)	2.1737(18)	2.159(6)	2.083(5)
Cu8–C4	2.167(12)	2.149(7)	2.155(5)	2.1361(17)	2.150(5)	1.984(5)
Cu3–C1	1.923(11)	1.924(7)	1.907(5)	1.9072(19)	1.915(4)	1.953(6)
Cu4–C2	1.937(11)	1.924(7)	1.920(5)	1.9265(18)	1.909(5)	1.947(6)
Cu5–C3	1.934(12)	1.913(8)	1.928(5)	1.9152(18)	1.909(6)	1.935(6)
Cu6–C4	1.935(11)	1.918(6)	1.909(5)	1.9187(17)	1.933(6)	1.968(6)
Cu3–O1	1.850(7)	1.854(5)	1.855(4)	1.8426(13)	1.841(3)	1.863(4)
Cu4–O1	1.848(7)	1.843(5)	1.834(4)	1.8355(13)	1.839(3)	1.851(4)
Cu5–O1	1.853(7)	1.848(5)	1.843(3)	1.8372(13)	1.833(3)	1.845(4)
Cu6–O1	1.847(7)	1.860(4)	1.853(4)	1.8413(12)	1.829(3)	1.863(4)

very small τ value at Cu1 is indicative of a square-pyramidal coordination sphere, while the coordination polyheders of the Cu2 and Cu7 ions are closer to a trigonal-bipyramidal geometry (Figure 7). One peripheral copper ion (Cu8) is only threefold coordinated and adopts a distorted “T-shape”, as evidenced by the bond angles C4–Cu8–N12 (172.1(2)°) and C4–Cu8–N15 (112.3(3)°; see Table S7). The N15–Cu8 bond is, as expected from the poor donor character of the N(CH₃)(quinolyl) group, very weak if present at all (2.711(6) Å; Table 2). If the Cu6···Cu8 binding contact (2.427(1) Å) is taken into account, a distorted-square-planar or tetrahedral environment is observed for this copper center. Closer inspection of the crystal packing of **8** reveals π – π interactions similar to those previously observed for **2** and [L⁶Cu]₄, which are, however, exceptional in this case. One noncoordinating quinolyl substituent of each complex molecule undergoes *intramolecular* π – π stacking with the adjacent mesityl group that also exhibits a weak *intermolecular* π – π contact with one coordinating quinolyl substituent of a second molecule of **8**. Remarkably, these interactions clearly affect the N-donor abilities of the quinolyl groups, thus resulting in very long Cu1–N4 bonding distances (2.454(5) Å) and nonbonding distances between Cu8 and N16 (3.034(6) Å). Overall, this gives rise to a dimeric arrangement which is held together by weak π – π stacking interactions in a molecular “gear rack” fashion (Figure 8). Again, L⁶ is responsible for the unusual structural features of **8** that originate from the combination of π – π stacking yet weakly coordinating donor side groups and the presence of aromatic organometallic ligands that are capable of supporting such π – π contacts.

A common structural feature and part of the general structural motif of 3–8 is represented by the pseudo tetrahedral

(μ_4 -O)Cu^I₄ core. As the Cu–O–Cu bond angles reveal, these central units deviate considerably from an ideal tetrahedral geometry. The largest differences are found in complex **4**, where those angles vary from 94.75(19) to 124.6(3)°. Similar distortion is also observed for the two (μ_4 -O)Cu^I₄ centers in [Cu₁₀O₂Mes₆]₁₀, whereas in Cu^{II} complexes of the type [L₄Cu^{II}₄(μ -O)X₆] (L = monodentate ligand, X = halide), bearing an isostructural core, the Cu–O–Cu bond angles are closer to the value expected for an ideal tetrahedron. This may be explained by the presence of the halide capping ligands in the Cu^{II} complexes, which additionally stabilize the tetrahedral coordination sphere.³⁰ Other Cu^{II} complexes of this type, which involve a tridentate phenolate bridging ligand instead of a monoligating donor group, also show a considerably distorted (μ_4 -O)Cu^{II}₄ unit (even though less distorted than that observed in 3–8), which is influenced by the steric constraints of the chelating ligand. As a consequence, the Cu–O–Cu angles opposite to the phenolate bridges are significantly smaller (about 103°), whereas the corresponding angles close to the halide bridges are substantially enlarged (110.1(2)–114.6(2)°).³¹ A similar observation was made for the molecular structures of the complexes [(μ_4 -O)Cu^I₄X₂(TMTCH)₄] (X = Cl, Br; TMTCH = 3,3,6,6-tetramethyl-1-thia-4-cycloheptyne). Herein, the two halide bridges cause the distortion by pulling two copper centers together.³² Although two pyrazolate capping ligands are present in 3–8, they do not affect the central (μ_4 -O)Cu^I₄ core in a similar way, since the mesityl bridges act as flexible “chain linkers” between the core and the peripheral binuclear pyrazolate frameworks. This is apparent from the bond angles Cu3–O1–Cu4 and Cu5–O1–Cu6 of 3–8, which lie opposite to the pyrazolate complex units, compared with the remaining “non-bridged”

Table 2. Selected Cu⋯Cu Distances (Å) and Bond Angles (deg) of 3–8

	3A	4A	5	6A	7	8
Cu1⋯Cu2	4.0000(22)	4.0121(15)	4.1671(9)	3.9982(7)	4.0598(7)	4.0420(11)
Cu7⋯Cu8	4.0418(32)	4.0145(9)	4.051(1)	4.0759(6)	4.1776(10)	3.783(1)
Cu3⋯Cu4	2.896(2)	2.9164(6)	3.0149(9)	2.8644(7)	3.0226(7)	2.8322(10)
Cu5⋯Cu6	2.939(2)	2.9106(14)	2.9129(9)	2.9105(5)	3.0790(7)	2.818(1)
Cu1–C1–Cu3	74.8(4)	74.5(2)	74.21(17)	75.57(7)	74.60(16)	75.1(2)
Cu2–C2–Cu4	72.9(4)	73.2(2)	73.85(17)	72.19(6)	74.29(16)	73.7(2)
Cu5–C3–Cu7	72.2(4)	72.8(3)	75.44(18)	72.44(6)	71.32(19)	74.94(19)
Cu6–C4–Cu8	72.6(4)	73.3(2)	73.53(17)	73.86(6)	71.31(19)	75.8(2)
Cu1–C1–C _p	113.18(44)	121.46(2)	116.0(3)	116.13(8)	112.8(2)	128.8(3)
Cu2–C2–C _p	129.36(46)	124.44(2)	117.7(3)	137.82(9)	115.5(2)	130.8(4)
Cu7–C3–C _p	129.49(49)	127.82(1)	119.7(2)	122.64(7)	128.2(3)	128.8(3)
Cu8–C4–C _p	116.09(44)	116.77(1)	120.2(2)	133.05(7)	127.7(2)	136.1(3)
Cu3–C1–C _p	171.88(52)	163.88(1)	169.7(3)	168.28(9)	172.4(2)	156.2(4)
Cu4–C2–C _p	157.74(52)	162.33(1)	168.4(3)	149.95(8)	170.2(2)	155.4(4)
Cu5–C3–C _p	161.28(57)	165.08(1)	164.9(3)	164.87(9)	160.4(3)	157.7(3)
Cu6–C4–C _p	171.28(52)	165.11(1)	166.2(3)	153.07(8)	159.6(3)	148.1(3)
C1–Cu3–O1	177.5(4)	174.0(3)	175.92(19)	173.17(7)	176.90(16)	168.2(2)
C2–Cu4–O1	174.2(4)	175.3(3)	177.44(19)	170.82(7)	177.01(16)	168.4(2)
C3–Cu5–O1	173.2(4)	175.6(2)	172.7(2)	172.39(7)	175.16(19)	170.4(2)
C4–Cu6–O1	177.7(4)	176.4(3)	176.99(19)	168.85(6)	173.19(18)	166.02(19)
Cu3–O1–Cu4	103.1(4)	104.2(2)	109.62(17)	102.30(6)	110.41(15)	99.40(17)
Cu3–O1–Cu5	106.8(4)	124.6(3)	107.18(18)	115.49(7)	103.71(15)	109.7(2)
Cu3–O1–Cu6	106.7(3)	94.75(19)	98.13(17)	113.99(7)	115.52(18)	100.86(18)
Cu4–O1–Cu5	117.8(4)	120.0(2)	117.6(2)	116.92(7)	111.61(18)	107.83(19)
Cu4–O1–Cu6	116.4(4)	105.2(2)	118.18(19)	103.23(6)	101.36(15)	138.4(2)
Cu5–O1–Cu6	105.2(4)	103.4(2)	104.02(17)	104.60(6)	114.46(15)	98.92(17)

Cu–O–Cu angles (Table 2). There is indeed a clear tendency of smaller angles in the first case for **6A** (with the exception of Cu4–O1–Cu6) and **8**, while in **3A**, **4A**, **5**, and **7** the differences are only small or exhibit no clear trend. Thus, the distortion of the $(\mu_4\text{-O})\text{Cu}_4^{\text{I}}$ tetrahedron seems to depend on packing effects in the crystal structures rather than on the influence of the respective capping ligand. The Cu–O bond distances of **3–8** are not significantly different from each other and lie in a range similar to that observed for $[\text{Cu}_{10}\text{O}_2\text{Mes}_6]$.¹⁰ They are, however, slightly shorter than in the complexes of the type $[(\mu_4\text{-O})\text{Cu}_4\text{X}_2(\text{TMTCH})_4]$ (averaged Cu–O bonding distances 1.908(3) Å) and also in comparison with the Cu–O bonds of cupric compounds $[(\mu_4\text{-O})\text{Cu}_4\text{X}_6\text{L}_4]$.^{30,32} This may be due to the higher coordination numbers at the copper centers in those latter complexes, since in the crystal structure of cuprite (Cu_2O), which consists of linear O–Cu–O units, short (1.848 Å) Cu–O bonding distances are also observed.³³ The linking Cu(μ -Mes)Cu units of all these complexes **3–8** show typical Cu–C bond lengths and Cu–C_i–Cu angles as well as Cu⋯Cu separations (Tables 1 and 2), which are also observed in the molecular structures of the parent $[\text{Cu}_{10}\text{O}_2\text{Mes}_6]$ and $[\text{Cu}_5\text{Mes}_5]$. In contrast to what is expected from these two examples, the bridging σ -mesityl ligands in **3–8** are rather asymmetric. This is evident from the considerably differing Cu(pz)–C(1–4) and Cu(O)–C(1–4) bond lengths. These differences lie in the range of 0.2–0.3 Å for **3–7** (but less than 0.2 Å in the case of **8**). Consequently, the mesityl groups lean toward the pyrazolate-ligated, peripheral Cu^I centers, as reflected by the relatively small Cu(pz)–C(1–4)–C_p angles and the substantially larger angles

Cu(O)–C(1–4)–C_p that are related to the $(\mu_4\text{-O})\text{Cu}_4^{\text{I}}$ core (Table 2). They differ in the range of about 40–50° for **3–5** and **7**. Notable exceptions are complex **6** and again **8** (up to 30°). Generally, all complexes **3–8** can thus be viewed as heteroleptic cuprate anions $[(\text{MesCu}^{\text{I}})_4(\mu_4\text{-O})]^{2-}$ that are flanked and stabilized by two capping $[(\text{L}^1\text{-L}^6)\text{Cu}^{\text{I}}_2]^+$ cations. This structural motif is very rare and is only known for few organocopper compounds such as the homoleptic 8-(dimethylamino)naphthylcopper(I).³⁴ It should also be noted that a heteroleptic cuprate anion involving oxygen as a coligand has not been reported in the literature so far. In principle, it might seem feasible to separate this anionic complex part from the attached $[(\text{L}^1\text{-L}^6)\text{Cu}^{\text{I}}_2]^+$ clamps. This was tried by employing ligand L^5H with the intention to obtain two separated $[(\text{L}^5)\text{Cu}^{\text{I}}_2]^+$ cations, in which both copper centers are tetrahedrally coordinated, and the free cuprate anion $[(\text{MesCu}^{\text{I}})_4(\mu_4\text{-O})]^{2-}$. Inspiration for this approach comes from the preparation method for $[(\text{DPPE})_2\text{-Cu}][\text{CuMes}_2]$, which was simply obtained by treating mesitylcopper with DPPE in an equimolar ratio in toluene. The X-ray structure determination indeed revealed separated $[(\text{DPPE})_2\text{-Cu}]^+$ and $[\text{CuMes}_2]^-$ ions.⁷ Also, more complex cuprate anions such as $[\text{Cu}_5\text{Ph}_6]^-$ and the recently reported tetrasilicide tetraanion $[(\text{MesCu})_2\text{Si}_4]^{4-}$ are known to be stable without contact ion pairing.^{35,36} As confirmed by the X-ray structure analysis of **7**, however, in the solid state the two additional pyridyl side arms of the pyrazolate ligands do not participate in coordination at all. Attempts to separate the binuclear pyrazolate-based complex cations from the central $[(\text{MesCu}^{\text{I}})_4(\mu_4\text{-O})]^{2-}$ core by slow heating of a solution of **7** in benzene-*d*₆ up to 70 °C, which was

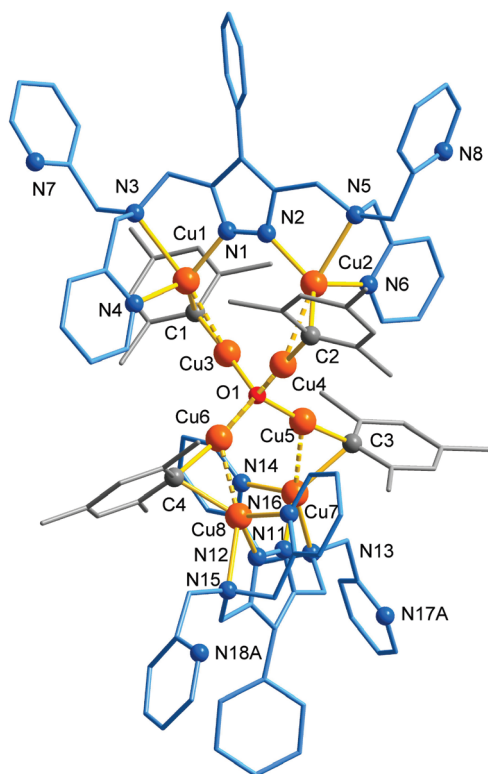


Figure 6. Molecular structure of 7. Hydrogen atoms have been omitted for clarity. Cu···Cu contacts are represented as dashed lines.

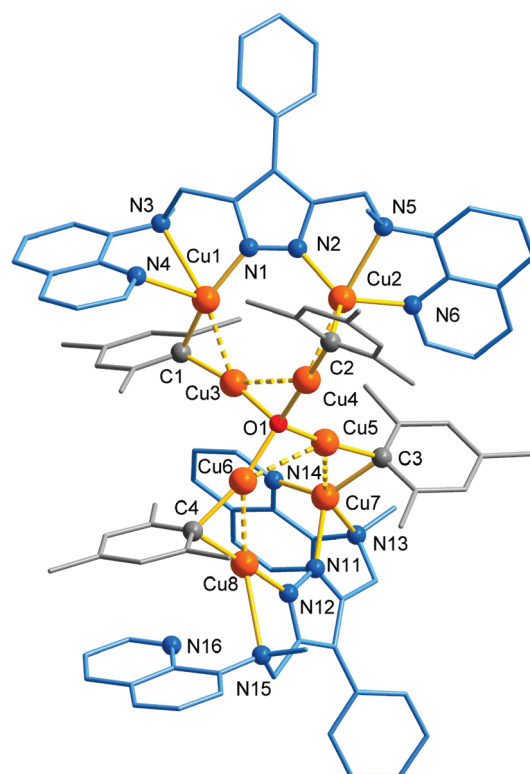


Figure 7. Molecular structure of 8. Hydrogen atoms have been omitted for clarity. Cu···Cu contacts are represented as dashed lines.

Table 3. τ Values of the $\{N_3\}Cu(\mu_2\text{-Mes})\cdots Cu$ Coordination Polyheders of 3–8

	3A	4A	5	6A	7	8
$\{N_3\}Cu1(\mu_2\text{-Mes})\cdots Cu3$	0.65	0.60	0.50	0.56	0.63	0.02
$\{N_3\}Cu2(\mu_2\text{-Mes})\cdots Cu4$	0.58	0.48	0.48	0.61	0.60	0.50
$\{N_3\}Cu7(\mu_2\text{-Mes})\cdots Cu5$	0.60	0.70	0.59	0.59	0.52	0.40
$\{N_3\}Cu8(\mu_2\text{-Mes})\cdots Cu6$	0.69	0.63	0.57	0.62	0.50	–

monitored by ^1H NMR, resulted in decomposition, as indicated by the presence of free ligand $L^5\text{H}$, a considerable amount of mesitylene, and unknown byproduct.

^1H NMR spectra of organocopper complexes 3–6 in benzene- d_6 are very similar: All compounds show only one set of the expected proton signals, thus supporting the presence of a symmetric arrangement in solution on the NMR time scale (see Table 4 and the Experimental Section). In comparison with their free ligands $L^1\text{H}$ – $L^6\text{H}$, some characteristic groups show significant shifts, especially those that are influenced by the coordinated metal centers, such as the pyridyl or quinolyl donor substituents. The most striking effects are the downfield shifts of the py H^6 protons by about 1.4–1.7 ppm. Similar observations are also made for the corresponding ^{13}C NMR data of 3–6. The spectra of complexes 7 and 8 exhibit basically the same trends, although the typical downfield shift for the py H^6 and quin H^2 protons, respectively, is smaller than for 3–6 (around 0.9 ppm). 7 also shows some broad resonances in the ^1H NMR spectrum that can be related to the pyridyl side arms which are only weakly coordinating at the Cu^1 ions of the compartmental ligand backbones or, as the molecular structure of 7 suggests, are not

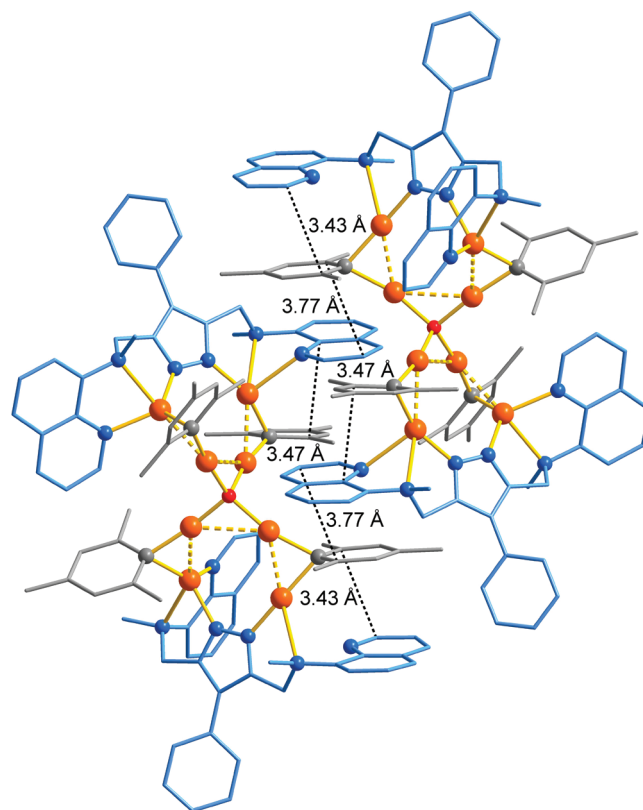


Figure 8. Representation of two complex molecules of the crystal structure of 8. Inter- and intramolecular π – π stacking is highlighted by selected close C···C distances.

Table 4. Selected ^1H and ^{13}C NMR Data for 3–8 (298 K, Benzene- d_6)

group	3	4	5	6	7	8
^1H NMR (δ)						
<i>o</i> -CH ₃	2.60 (s)	2.60 (s)	2.57 (s)	2.60 (s)	2.72 (s)	2.52 (s)
<i>p</i> -CH ₃	2.20 (s)	2.25 (s)	2.25 (s)	2.28 (s)	2.22 (s)	2.08 (s)
<i>m</i> -Mes	6.78 (s)	6.83 (s)	6.79 (s)	6.85 (s)	6.88 (s)	6.48 (s)
pz CH ₂	3.32 (s)	3.49 (s)	3.44, 3.54 (s)	3.74 (s)	3.90 (s)	4.16 (s)
py CH ₂	3.15 (s)	2.97 (s)	3.44, 3.54 (s)	3.29 (s)	3.52 (s)	
pz H ⁴	5.95 (s)	—	5.98 (s)	—	—	—
py H ³	6.39 (d) ($^3J_{\text{HH}} = 7.7$ Hz)	6.31 (d) ($^3J_{\text{HH}} = 7.6$ Hz)	6.38–6.40 (m)	6.29–6.31 (m)	6.61 (d) ($^3J_{\text{HH}} = 7.7$ Hz)	—
py H ⁴ /quin H ⁴	6.89 (dt) ($^4J_{\text{HH}} = 1.7$, $^3J_{\text{HH}} = 7.6$ Hz)	6.89 (dt) ($^4J_{\text{HH}} = 1.7$, $^3J_{\text{HH}} = 7.6$ Hz)	6.90–6.95 (m)	6.91–6.96 (m)	6.92 (dt) ($^4J_{\text{HH}} = 1.8$, $^3J_{\text{HH}} = 7.6$ Hz)	7.43 (dd) ($^4J_{\text{HH}} = 1.2$, $^3J_{\text{HH}} = 8.3$ Hz)
py H ⁵ /quin H ³	6.74–6.76 (m)	6.77–6.80 (m)	6.90–6.95 (m)	6.91–6.96 (m)	6.67–6.72 (m)	6.72–6.76 (m)
py H ⁶ /quin H ²	9.89 (d) ($^3J_{\text{HH}} = 4.4$ Hz)	10.07 (d) ($^3J_{\text{HH}} = 4.3$ Hz)	9.98–9.99 (m)	10.05–10.06 (m)	9.23–9.25 (m)	9.27–9.28 (m)
^{13}C NMR (δ)						
<i>o</i> -CH ₃	29.6	29.7	29.6	29.7	29.8	29.8
<i>p</i> -CH ₃	21.5	21.6	21.7	21.7	21.5	21.5
<i>m</i> -Mes	124.4	124.4	124.7	124.8	124.8	124.6
pz CH ₂	56.2	55.6	51.5, 54.8	50.7	51.2	57.3
py CH ₂	61.2	61.1	51.5, 54.8	54.6	57.2	
pz C ⁴	97.7	115.2	97.8	115.4	115.6	115.0
py C ³	122.3	122.2	121.6	121.5	123.6	
py C ⁴ /quin C ⁴	135.8	135.8	135.9	136.0	135.7	135.7
py C ⁵ /quin C ³	123.0	123.1	122.7	122.7	122.4	119.5 or 122.0
py C ⁶ /quin C ²	147.1	152.3	151.7	151.8	150.8	150.1

involved in coordination at all. Extreme line broadening prevents detection of a complete signal set of one of those groups or an exact assignment of corresponding single resonance signals (see the Experimental Section). It might be expected that elevated temperatures should result in a higher population of noncoordinating pyridyl side groups in solution, which would also lead to decreasing line broadening of the corresponding ^1H NMR resonances. As already mentioned, under these conditions, however, only decomposition of complex 7 could be observed. Complex 8 represents again an exception from this series of organocopper frameworks, since a minor product (or a mixture of different species) is observed both in the ^1H and the ^{13}C NMR spectra. The overall amount of this (these) side product(s) lie(s) in the range of about 5–10%, related to the major species. Since the additional resonance signals were observed in spectra from different samples obtained under altered conditions—even from single-crystal material—and since no free pyrazolate ligand is observed, simple decomposition of 8 in solution can be ruled out. Due to the fact that the intensities of the additional signals are very low, at this stage the identity of this (these) minor species remain(s) unknown. It seems likely, however, that the hemilabile character of L^6 is responsible for the formation of different isomers of 8, which differ only by the number of $\text{CH}_2\text{N}(\text{CH}_3)(8\text{-quinolyl})$ side arms that are either coordinating or dangling. This is supported not only by the known fluxional behavior of these side groups¹⁵ but also by the unusual structural characteristics of 8 in the solid state (vide supra).

Structural Features of 1 and 2 Compared with Those of 5 and 8. As described above, the binuclear Cu^{I} complexes 1 and 2

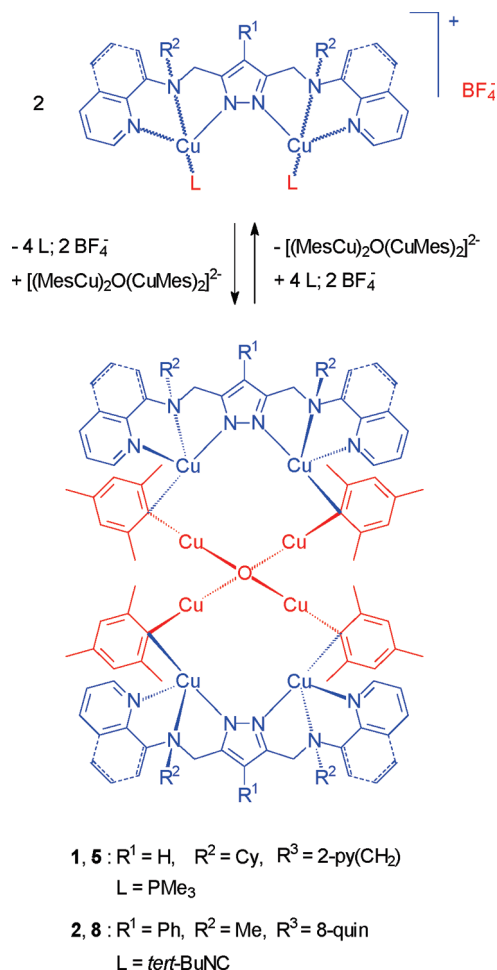
exhibit different stereochemical arrangements in the solid state which can be viewed as *cis/trans* isomers, if the position of the ancillary ligands PMe_3 and $t\text{BuNC}$ relative to the plane defined by the central pyrazolate heterocycle is considered (Figures S3 and S6, Supporting Information). This can also be analyzed for the binuclear Cu^{I} pyrazolate scaffolds of the organocopper species 3–8. The most informative examples are 5 and 8, since these complexes can be directly compared with their binuclear counterparts 1 and 2, which contain the same pyrazolate compartmental ligands. In all examples with the exception of 8, the positions of the ipso carbon atoms of the two mesityl bridges at each binuclear complex unit relative to the pyrazolate plane confirm a *trans* orientation of both σ -organo ligands (shown for 5 in Figure S11).

Such a *trans* orientation of the σ -mesityl ligands is observed at both binuclear Cu^{I} pyrazolate units within each complex, which represent a pair of the two enantiomers *trans* and *trans'*. This arrangement is determined by the pseudotetrahedral $(\mu_4\text{-O})\text{Cu}_4^{\text{I}}$ cluster, which obviously allows no structural alternatives that could provide less steric hindrance. In the solid-state molecular structure of complex 8 only one binuclear cap of the molecule exhibits the *trans* configuration of the σ -mesityl groups (the alternative *trans'* form is shown in Figure S17). As a result of extended π – π -stacking interactions and the hemilabile character of the quinolyl groups, one such group does not coordinate at the second L^6Cu_2 cap and therefore no *cis/trans* isomerism is observed there.

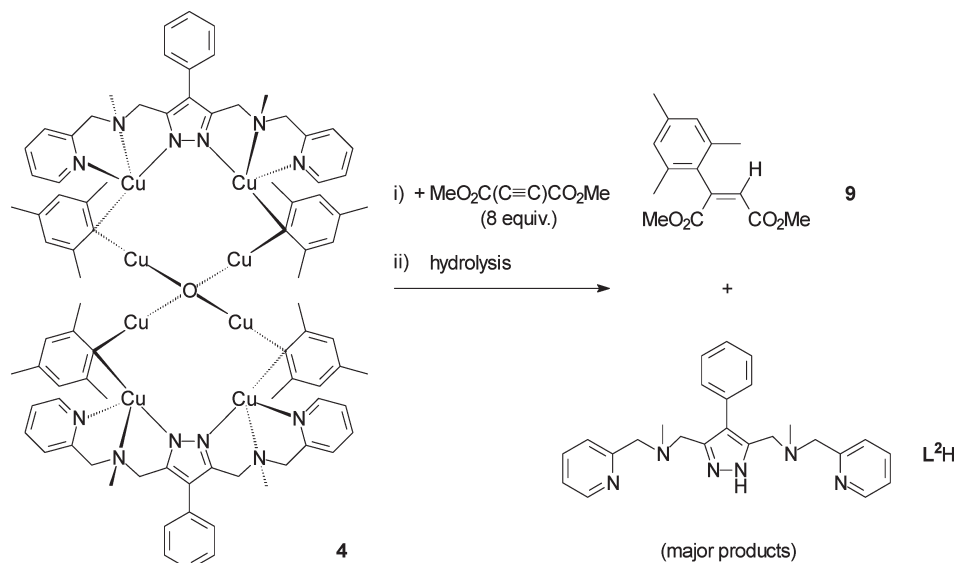
More striking is a comparison of the structural features regarding the cuprocuprate character of 3–8 with those of their

related binuclear complexes. For example, if both the monodentate coligands and the anionic counterion BF_4^- of **1** or **2** are

Scheme 3. Structural Relation between 1 and 5 as well as 2 and 8



Scheme 4. Reaction of Complex 4 with DMADC



formally substituted by $[(\text{MesCu}^{\text{I}})_4(\mu_4\text{-O})]^{2-}$, the organocupper complexes **5** and **8** are obtained (Scheme 3).

Thus, the complex cations $[\text{L}^3\text{Cu}_2^{\text{I}}]^+$ and $[\text{L}^6\text{Cu}_2^{\text{I}}]^+$, which are isolable as their ionic complexes **1** and **2**, are clearly supportive of the cuprate features particularly of **5** and **8**, but also generally for the complete series **3–8** of this type of organo-copper complexes that follow a common structural motif.

Reaction of Complex 4 with Dimethyl Acetylenedicarboxylate (DMADC). The structural characteristics of **3–8** give rise to the question whether these complexes would undergo transformations typical for organocuprates. It has been earlier demonstrated by van Koten et al. that 8-(dimethylamino)naphthyl-copper(I) exhibits remarkable cuprate features, since its reaction with the activated alkyne DMADC results in the syn-addition product $\text{Me}_2\text{N}(\text{naphthyl})\text{C}(\text{CO}_2\text{Me})=\text{C}(\text{CO}_2\text{Me})\text{H}$ after hydrolysis.³⁴ This is quite unusual, since typically only lithium and magnesium cuprates show similar reactivity. Complex **4** was thus chosen as a representative example and was reacted with an excess (8 equiv) of DMADC, as outlined in Scheme 4.

After workup, a viscous yellow oil was obtained and analyzed by ^1H NMR spectroscopy as a mixture of the addition product **9** (1.2 equiv) and the liberated pyrazole ligand L^2H (1 equiv), as well as traces of unidentified byproduct. **9** is characterized by two singlets in the ^1H NMR spectrum in d_6 -benzene at δ 2.05 and 2.33 ppm for the mesityl CH_3 protons, two OCH_3 signals at δ 3.33 and 3.41 ppm, the olefinic proton resonance at δ 5.77 ppm, and a multiplet between δ 6.69 and 6.70 ppm for the mesityl CH groups. Its presence is also confirmed by an EI mass spectrum of the product mixture, which shows fragments of **9** as well as its molecular ion peak at m/z 262. This shows that **4** (and presumably all other complexes **3–8**) can transfer a σ -mesityl group onto activated alkynes. The considerable amount of L^2H suggests that the original complex framework of **4** is completely degraded during this reaction, at least in the organic phase after hydrolytic workup.

CONCLUSIONS

In conclusion, we have elaborated a convenient method to synthesize the two new Cu^{I} complexes **1** and **2** with pyrazolate-based

compartmental ligands. Together with the X-ray crystal structure determination of such a ligand system bearing $\{N_2\}$ side arms, **1** and **2** have been presented as the first examples of binuclear Cu^I pyrazolates of the type $[LCu_2]X$. In solution these complexes interconvert between different isomers, and in the case of **2** remarkable structural features originate from the hemilabile character of the $-CH_2N(Me)(8\text{-quinolyl})$ side groups and their capability to undergo $\pi-\pi$ stacking interactions.

Second, it could be shown that L^1H-L^6H , 4 equiv of mesitylcopper and $1/4$ equiv of dioxygen form a series of unusually stable organocopper assemblies **3–8** of general composition $[(L^1-L^6)Cu_2(\mu_2\text{-MesCu})_2(\mu_4\text{-O})(\mu_2\text{-MesCu})_2(L^1-L^6)Cu_2]$, all with the same basic structural motif. Structural details of the peripheral $\{(L^1-L^6)Cu_2\}$ fragments of **3–8** are closely related to those of complexes **1** and **2**. Indeed, the observation of differing $Cu-C_{ipso}$ bonding distances within the organocopper core of **3–8** is strong evidence for a cuprocuprate arrangement consisting of two $[(L^1-L^6)Cu_2]^+$ cations that serve as capping (thus stabilizing) units for the complex heteroleptic O-centered cuprate anion $[(MesCu)_4(\mu_4\text{-O})]^{2-}$. Subtle differences in the solid-state structures of **3–8** are induced by the different chelate arms of the peripheral ligand scaffolds L^1-L^6 , and intriguing structural relations between the cap groups $[(L^1-L^6)Cu_2]^+$ and the analogous complexes **1** and **2** are apparent; these features are strongly influenced by the hemilabile nature of the quinolyl side arms and their ability to undergo extended $\pi-\pi$ stacking interactions in the solid state.

Finally, as demonstrated in the case of **4**, these organocopper assemblies show unusual reactivity toward activated alkynes such as DMADC. Their σ -mesityl groups are predominantly transferred to the activated alkyne, resulting in the addition product **9**, which is believed to be formed via a syn addition.

Interesting chemistry obviously arises from the combination of established organometallic synthons and compartmental ligand scaffolds originally developed for biomimetic/bioinspired metal complexes. To explore other useful transformations with the versatile cuprate frameworks reported here and to generate other oligonuclear copper species by activating small molecules apart from dioxygen are of ongoing interest in our current and future research projects.

EXPERIMENTAL SECTION

General Procedures. All manipulations involving Cu^I compounds were carried out by using Schlenk techniques under an atmosphere of dry argon. Glassware and NMR tubes were heat-sealed with a heat gun under vacuum. Prior to use, tetrahydrofuran (THF), diethyl ether, toluene, and pentane were freshly distilled from sodium/benzophenone. Benzene- d_6 and tetrahydrofuran- d_8 were distilled from sodium. Dichloromethane was dried over calcium hydride and distilled. Acetonitrile and propionitrile were dried over phosphorus pentoxide and distilled. Ethanol was dried according to the established method via sodium/diethyl phthalate.³⁷ $KOtBu$ (Acros), $NaN(SiMe_3)_2$ (2 M solution in THF, Alfa Aesar), $tBuNC$ (Aldrich), PMe_3 (1 M in THF, Aldrich), N -(2-picolyl)cyclohexylamine (ABCRCR), and dimethyl acetylenedicarboxylate (DMADC, Aldrich) were used as purchased. $[Cu(CH_3CN)_4]BF_4$,³⁸ N -(2-picolyl)methylamine,^{11,39} and N -bis(2-picolyl)amine⁴⁰ were prepared according to the literature procedures. The syntheses of 3,5-bis(chloromethyl)-1-(tetrahydropyran-2-yl)pyrazole,^{18,20b} 3,5-bis(chloromethyl)-1-(tetrahydropyran-2-yl)-4-phenylpyrazole,¹¹ L^2H ,¹¹

L^6H ,¹⁵ and 4^{11} were described previously. Mesitylcopper was synthesized according to a known procedure.^{6c}

Elemental analyses were performed by the Analytical Laboratory of the Institute for Inorganic Chemistry at the University of Göttingen (Elementar Vario EL III). Melting points for L^3H and L^4H were determined with an SRS (Stanford Research Systems) Opti Melt instrument; values are uncorrected. NMR measurements were performed at 300 K on a Bruker AC 200 at 200.13 MHz (1H) and 50.33 MHz (^{13}C), a Bruker Avance 300 at 300.13 MHz (1H) and 75.47 MHz (^{13}C), and a Bruker Avance 500 at 500.13 (1H), 125.77 (^{13}C), and 202.46 MHz (^{31}P), respectively. ^{13}C NMR resonances were obtained with proton broad-band decoupling and referenced to the solvent signals of benzene- d_6 at 128.0 ppm, THF- d_8 at 25.3 ppm, and chloroform at 77.0 ppm (1H NMR residual nondeuterated and partially deuterated solvent signals, 7.15 (benzene- d_6), 1.73 (THF- d_8), and 7.24 ppm ($CDCl_3$), respectively). Most assignments are based on H,H and C,H correlation experiments. EI-MS spectra were recorded on a Finnigan MAT 8200 instrument and ESI-MS spectra on an Applied Biosystems API 2000 as well as on a Thermo Finnigan Ion Trap LCQ spectrometer. ESI-HRMS, performed by using a Bruker FTICR APEX IV instrument, was applied for compounds whose accurate elemental analyses were difficult to obtain or as supplemental data.

L^1H .⁴¹ A suspension of anhydrous Na_2CO_3 (3.973 g, 37.48 mmol), 3,5-bis(chloromethyl)-1-(tetrahydropyran-2-yl)pyrazole (0.935 g, 3.75 mmol), and N -(2-picolyl)methylamine (0.919 g, 7.52 mmol) in acetonitrile (80 mL) was heated to reflux for 36 h, then cooled to room temperature and subsequently filtered. Evaporation of the solvent gave an oily orange residue that was treated dropwise with ethanolic HCl (40 wt %, 6 mL) and diethyl ether (50 mL). The resulting suspension was stirred for 2 h. The precipitate was separated by filtration, washed with diethyl ether (6×60 mL), and dried in vacuo for 1 h. After addition of aqueous KOH (pH 12, 80 mL) the product was extracted with CH_2Cl_2 (5×40 mL). The combined organic phases were dried with $MgSO_4$. Filtration and evaporation of the solvent afforded a golden viscous oil which was dried in vacuo overnight. Yield: 0.973 g (2.89 mmol, 77%). 1H NMR (300.13 MHz, $CDCl_3$): δ 2.28 (s, 6 H, CH_3), 3.63, 3.66 (2 \times s, 8 H, py and pz CH_2), 6.16 (s, 1 H, pz H^4), 7.15 (ddd, $^4J_{HH} = 1.1$ Hz, $^3J_{HH} = 4.9$ Hz, $^3J_{HH} = 7.5$ Hz, 2 H, py H^5), 7.40 (d, $^3J_{HH} = 7.8$ Hz, 2 H, py H^3), 7.63 (dt, $^4J_{HH} = 1.8$ Hz, $^3J_{HH} = 7.7$ Hz, 2 H, py H^4), 8.54 (ddd, $^5J_{HH} = 0.9$ Hz, $^4J_{HH} = 1.7$ Hz, $^3J_{HH} = 4.9$ Hz, 2 H, py H^6). ^{13}C NMR (125.77 MHz, $CDCl_3$): δ 42.5 (CH_3), 52.9 (broad, 62 (CH_2), 105.1 (CH , pz C^4), 122.1 (CH , py C^5), 123.6 (CH , py C^3), 136.5 (CH , py C^4), ~ 145.0 (br, C, pz $C^{3,5}$), 149.0 (CH , py C^6), 158.7 (C, py C^2). MS (ESI(+) in MeOH): m/z (relative intensity) 337.21 (100) $[M + H]^+$. HRMS (ESI(+) in MeOH): m/z calcd for $C_{19}H_{25}N_6$ $[M + H]^+$ 337.214 07, found 337.213 53.

L^3H . This compound was prepared according to the method described for L^1H by the use of Na_2CO_3 (5.560 g, 52.46 mmol), 3,5-bis(chloromethyl)-1-(tetrahydropyran-2-yl)pyrazole (1.310 g, 5.26 mmol), and N -(2-picolyl)cyclohexylamine (2.000 g, 10.51 mmol), which were heated in solution to reflux for 48 h. The crude product was purified by column chromatography (basic alumina, 1:0 to 10:1 v/v ethyl acetate/methanol). A colorless solid was obtained and dried in vacuo for 24 h. Yield: 1.172 g (2.48 mmol, 47%). Mp: 112 °C. Anal. Calcd for $C_{29}H_{40}N_6$: C, 73.69; H, 8.53; N, 17.78. Found: C, 73.08; H, 8.80; N, 17.45. 1H NMR (300.13 MHz, C_6D_6): δ 0.83–1.20 (m, 10 H, cy H^{2a-4a}), 1.39–1.44 (m, 2 H, cy H^{4e}), 1.57–1.61 (m, 4 H, cy H^{3e}), 1.80–1.84 (m, 4 H, cy H^{2e}), 2.53–2.62 (m, 2 H, cy H^1), 3.81, 3.91 (2 \times s, 8 H, py and pz CH_2), 6.33 (s, 1 H, pz H^4), 6.61 (ddd, $^4J_{HH} = 1.1$ Hz, $^3J_{HH} = 4.9$ Hz, $^3J_{HH} = 7.4$ Hz, py H^5), 7.10–7.14 (m, 2 H, py H^4), ~ 7.39 –7.42 (m, broad, 2 H, py H^3), 8.39–8.41 (m, 2 H, py H^6). 1H NMR (500.13 MHz, THF- d_8): δ 1.03–1.18 (m, 6 H, cy $H^{3a,4a}$), 1.30 (dq, $^3J_{HaHe} = 2.8$ Hz, $^2J_{HaHe}$, $^3J_{HaHa'} = 11.9$ Hz, 4 H, cy H^{2a}), 1.54–1.56 (m, 2 H, cy H^{4e}), 1.71–1.72 (m, 4 H, cy H^{3e}), 1.84–1.87 (m, 4 H, cy H^{2e}), 2.50 (tt, $^3J_{HaHa} = 3.4$ Hz, $^3J_{HaHa'} = 11.5$ Hz, 2 H, cy H^1), 3.68, 3.78

(2 × s, 8 H, py and pz CH₂), 6.11 (s, 1 H, pz H⁴), 7.05 (ddd, ⁴J_{HH} = 1.6 Hz, ³J_{HH} = 4.8 Hz, ³J_{HH} = 6.7 Hz, 2 H, py H⁵), 7.53–7.58 (m, 4 H, py H^{3,4}), 8.39–8.40 (m, 2 H, py H⁶). ¹³C NMR (75.47 MHz, C₆D₆): δ 26.3 (CH₂, cy C³), 26.5 (CH₂, cy C⁴), 29.4 (CH₂, cy C²), 47.6 (broad), 56.3 (py and pz CH₂), 60.0 (CH, cy C¹), 103.2 (CH, pz C⁴), 121.6 (CH, py C⁵), 122.6 (CH, py C³), 136.0 (CH, py C⁴), 149.1 (CH, py C⁶), 162.2 (C, py C²). The signal of pz C^{3,5} is too broad to be detected. ¹³C NMR (125.77 MHz, THF-*d*₈): δ 27.0 (CH₂, cy C³), 27.3 (CH₂, cy C⁴), 29.8 (CH₂, cy C²), 47.8 (broad), 56.7 (py and pz CH₂), 60.3 (CH, cy C¹), 103.9 (CH, pz C⁴), 122.1 (CH, py C⁵), 123.0 (CH, py C³), 136.6 (CH, py C⁴), ~147 (br, C, pz C^{3,5}), 149.4 (CH, py C⁶), 162.8 (C, py C²). MS (EI): *m/z* (relative intensity) 472 (1) [M]⁺, 380 (100) [M – (C₆H₆N)]⁺, 284 (19) [M – (C₆H₆N)(C₆H₁₁N) + H]⁺, 283 (14) [M – (C₆H₆N)(C₆H₁₁N)]⁺, 191 (32) [M – (C₆H₆N)(C₆H₁₁N) – (C₆H₆N)]⁺, 93 (21) [C₆H₇N]⁺. HRMS (ESI(+)) in MeOH): *m/z* calcd for C₂₉H₄₁N₆ [M + H]⁺ 473.339 27, found 473.339 07.

L⁴H. This compound was prepared according to the method described for L¹H by the use of Na₂CO₃ (5.315 g, 50.15 mmol), 3,5-bis(chloromethyl)-1-(tetrahydropyran-2-yl)-4-phenylpyrazole (1.608 g, 4.94 mmol), and *N*-(2-picolyl)cyclohexylamine (1.885 g, 9.91 mmol), which were heated in solution to reflux for 90 h. Recrystallization from diethyl ether and drying in vacuo for 15 h gave a beige powder. Yield: 1.010 g (1.84 mmol, 37%). Mp: 127 °C. Anal. Calcd for C₃₅H₄₄N₆: C, 76.60; H, 8.08; N, 15.31. Found: C, 75.93; H, 8.13; N, 15.00. ¹H NMR (500.13 MHz, C₆D₆): δ 0.81–0.88 (m, 2 H, cy H^{4a}), 0.92–1.12 (m, 8 H, cy H^{3a,2a}), 1.39 (d, ⁴J_{HH} = 12.3 Hz, 2 H, cy H^{4e}), 1.54 (d, ⁴J_{HH} = 12.3 Hz, 2 H, cy H^{3e}), ~1.71–1.72 (m, broad, 4 H, cy H^{2e}), ~2.50–2.55 (m, broad, 2 H, cy H¹), 3.92 (broad), 3.94 (2 × s, 8 H, py and pz CH₂), 6.56 (dd, ³J_{HH} = 4.9 Hz, ³J_{HH} = 8.2 Hz, 2H, py H⁵), 7.04 (t, ³J_{HH} = 6.4 Hz, 2 H, py H⁴), ~7.15 (m, broad, overlaid by the benzene signal, 2 H, py H³), 7.15–7.19 (m, overlaid by the benzene signal, 1 H, *p*-Ph), 7.29–7.33 (m, 2 H, *m*-Ph), 7.61–7.63 (m, 2 H, *o*-Ph), 8.36–8.37 (m, 2 H, py H⁶). ¹³C NMR (125.77 MHz, C₆D₆): δ 26.4 (CH₂, cy C³), 26.5 (CH₂, cy C⁴), 29.2 (CH₂, cy C²), 46.8 (broad), 56.2 (py and pz CH₂), 60.5 (CH, cy C¹), 118.7 (C, pz C⁴), 121.5 (CH, py C⁵), 122.7 (CH, py C³), 126.3 (CH, *p*-Ph), 128.5 (CH, *m*-Ph), 130.3 (CH, *o*-Ph), 135.2 (C, *i*-Ph), 135.9 (CH, py C⁴), 149.1 (CH, py C⁶), 162.1 (C, py C²). The signal of pz C^{3,5} is too broad to be detected. MS (EI): *m/z* (relative intensity) 548 (1) [M]⁺, 456 (100) [M – (C₆H₆N)]⁺, 360 (24) [M – (C₆H₆N)(C₆H₁₁N) + H]⁺, 359 (17) [M – (C₆H₆N)(C₆H₁₁N)]⁺, 267 (12) [M – (C₆H₆N)(C₆H₁₁N) – (C₆H₆N)]⁺, 266 (51) [M – (C₆H₆N)(C₆H₁₁N) – (C₆H₆N) – H]⁺, 191 (25) [M – (C₆H₆N)(C₆H₁₁N) – (C₆H₆N) – (C₆H₅) + H]⁺, 93 (31) [C₆H₇N]⁺. HRMS (ESI(+)) in MeOH): *m/z* calcd for C₃₅H₄₅N₆ [M + H]⁺ 549.370 57, found 549.370 13.

L⁵H. This compound was prepared according to the method described for L¹H by the use of Na₂CO₃ (4.410 g, 41.61 mmol), 3,5-bis(chloromethyl)-1-(tetrahydropyran-2-yl)-4-phenylpyrazole (1.350 g, 4.15 mmol), and *N*-bis(2-picolyl)amine (1.650 g, 8.28 mmol), which were heated in solution to reflux for 48 h. The resulting oily residue was dried in vacuo (5 × 10^{−4} mbar, 100 °C). A beige to brownish resin was obtained. Yield: 1.354 g (2.39 mmol, 58%). ¹H NMR (500.13 MHz, C₆D₆): δ 3.91 (s, broad, 12 H, CH₂), 6.55 (ddd, ⁴J_{HH} = 0.9 Hz, ³J_{HH} = 4.9 Hz, ³J_{HH} = 7.4 Hz, 4 H, py H⁵), 7.02 (dt, ⁴J_{HH} = 1.5 Hz, ³J_{HH} = 7.6 Hz, 4 H, py H⁴), 7.11–7.14 (m, 1 H, *p*-Ph), 7.18–7.21 (m and overlaid broad band, 6 H, py H³, *m*-Ph), 7.45–7.48 (m, 2 H, *o*-Ph), 8.35 (d, ³J_{HH} = 4.3 Hz, 4 H, py H⁶). ¹³C NMR (125.77 MHz, C₆D₆): δ 49.7 (broad), 59.8 (CH₂), 120.0 (C, pz C⁴), 121.7 (CH, py C⁵), 123.4 (CH, py C³), 126.2 (CH, *p*-Ph), 128.5 (CH, *m*-Ph), 130.3 (CH, *o*-Ph), 134.6 (C, *i*-Ph), 135.9 (CH, py C⁴), 149.2 (CH, py C⁶), 159.8 (C, py C²). The signal of pz C^{3,5} is too broad to be detected. MS (EI): *m/z* (relative intensity) 566.3 (1) [M]⁺, 474.2 (37) [M – (C₆H₆N)]⁺, 369.1 (12) [M – (C₁₂H₁₂N₃) + H]⁺, 275.0 (12) [M – (C₁₂H₁₂N₃) – (C₆H₆N) – H]⁺, 92.9 (100) [C₆H₇N]⁺. HRMS (ESI(+)) in MeOH): *m/z* calcd for C₃₅H₃₅N₈ [M + H]⁺ 567.298 47, found 567.298 08.

L⁶H. ¹⁵N NMR (500.13 MHz, C₆D₆): δ 2.84 (s, broad, 6 H, CH₃), 4.82 (s, broad, 4 H, CH₂), 6.73 (dd, ³J_{HH} = 4.1 Hz, ³J_{HH} = 8.2 Hz, 2 H, quin H³), 6.81 (d, broad, ³J_{HH} = 7.2 Hz, 2 H, quin H⁷), 6.91–6.94 (m, 1 H, *p*-Ph), 6.96–7.00 (m, 2 H, *m*-Ph), 7.02 (dd, ⁴J_{HH} = 1.2 Hz, ³J_{HH} = 8.1 Hz, 2 H, quin H⁵), 7.12–7.15 (m, overlaid by the benzene signal, 2 H, quin H⁶), 7.25–7.27 (m, 2 H, *o*-Ph), 7.52 (dd, ⁴J_{HH} = 1.8 Hz, ³J_{HH} = 8.3 Hz, 2 H, quin H⁴), ~8.41 (m, broad, 2 H, quin H²). ¹³C NMR (125.77 MHz, C₆D₆): δ 40.1 (broad, CH₃), 51.6 (CH₂), 116.2 (CH, quin C⁷), 120.0 (CH, quin C⁵), 120.7 (C, pz C⁴), 120.7 (CH, quin C³), 126.1 (CH, *p*-Ph), 126.9 (CH, quin C⁶), ~128.0 (CH, overlaid by benzene signal, *m*-Ph), 130.0 (C, quin C^{4a}), 130.3 (CH, *o*-Ph), 133.9 (C, *i*-Ph), 136.3 (CH, quin C⁴), 143.1 (C, quin C^{8a}), 147.3 (CH, quin C²), 149.5 (C, quin C⁸). The signal of pz C^{3,5} is too broad to be detected.

1. A solution of L³H (199 mg, 0.42 mmol) in THF (10 mL) was treated dropwise with a 2 M solution of Na(N(SiMe₃)₂) in THF (0.21 mL, 0.42 mmol). After it was stirred for 5 min, this solution was added to a suspension of [Cu(CH₃CN)₄]BF₄ (264 mg, 0.84 mmol) in THF (20 mL). After this mixture was stirred for 22 h, a 1 M solution of PMe₃ in THF (0.84 mL, 0.84 mmol) was added. The suspension was stirred for 6 days, then filtered over Kieselgur, and the resulting clear yellow to orange solution was concentrated in vacuo to 5 mL. Slow diffusion of diethyl ether (15 mL) into the solution at 4 °C over the course of 11 days afforded small pale yellow crystals. The orange solution was decanted, and the crystalline solid was washed with cold diethyl ether and then dried in vacuo for 18 h. Yield: 150 mg (0.18 mmol, 43%). Anal. Calcd for C₃₅H₅₇N₆P₂Cu₂BF₄: C, 50.18; H, 6.86; N, 10.03. Found: C, 49.74; H, 6.98; N, 9.78. ¹H NMR (500.13 MHz, C₆D₆): δ 0.77–1.02 (m, 10 H, cy H^{2a–4a}), 1.27 (d, ²J_{HP} = 5.9 Hz, 18 H, PMe₃), 1.38–1.42 (m, 2 H, cy H^{4e}), 1.48–1.50 (m, 4 H, cy H^{3e}), 1.72–1.75 (m, 4 H, cy H^{2e}), 2.41–2.45 (m, 2 H, cy H¹), 3.37, 3.65 (2 × s, broad, 8 H, py and pz CH₂), 6.00 (s, 1 H, pz H⁴), 6.43 (d, ³J_{HH} = 7.8 Hz, 2 H, py H³), 7.12–7.15 (m, overlaid by the benzene signal, 2 H, py H⁴), 7.49–7.51 (m, 2 H, py H⁵), 9.14 (d, ³J_{HH} = 4.8 Hz, 2 H, py H⁶). ¹H NMR (after 8 weeks, 500.13 MHz, C₆D₆): δ 0.80–1.07 (m, 10 H, cy H^{2a–4a}), 1.26 (d, ²J_{HP} = 5.8 Hz, 18 H, PMe₃), 1.37–1.42 (m, 2 H, cy H^{4e}), 1.50–1.52 (m, 4 H, cy H^{3e}), 1.76–1.78 (m, 4 H, cy H^{2e}), 2.43–2.48 (m, 2 H, cy H¹), 3.43, 3.65 (2 × s, broad, 8 H, py and pz CH₂), 5.98 (s, 1 H, pz H⁴), 6.60 (d, ³J_{HH} = 7.7 Hz, 2 H, py H³), 7.27 (t, ³J_{HH} = 7.4 Hz, 2 H, py H⁴), 7.49–7.52 (m, 2 H, py H⁵), 9.00–9.01 (m, 2 H, py H⁶). ¹H NMR (500.13 MHz, THF-*d*₈): δ 1.05–1.41 (m, 10 H, cy H^{2a–4a}), 1.28 (d, ²J_{HP} = 5.8 Hz, 18 H, PMe₃), 1.57–1.60 (m, 2 H, cy H^{4e}), 1.73–1.76 (m, overlaid by the THF signal, 4 H, cy H^{3e}), 2.00–2.03 (m, 4 H, cy H^{2e}), 2.67–2.72 (m, 2 H, cy H¹), 3.77, 3.83 (2 × s, broad, 8 H, py and pz CH₂), 5.71 (s, 1 H, pz H⁴), 7.29 (d, ³J_{HH} = 7.5 Hz, 2 H, py H³), 7.38–7.41 (m, 2 H, py H⁵), 7.72 (t, ³J_{HH} = 7.4 Hz, 2 H, py H⁴), 8.66–8.67 (m, 2 H, py H⁶). ¹³C NMR (125.77 MHz, C₆D₆): δ 16.5 (d, ¹J_{CP} = 20.9 Hz, CH₃, PMe₃), 26.0 (CH₂, cy C³), 26.2 (CH₂, cy C⁴), 29.9 (broad, CH₂, cy C²), 52.5, 55.2 (py and pz CH₂), 64.4 (CH, cy C¹), 98.3 (CH, pz C⁴), 121.7 (CH, py C⁵), 124.6 (CH, py C³), 137.2 (C, py C⁴), 149.2 (C, pz C^{3,5}), 151.2 (CH, py C⁶), 158.5 (C, py C²). ¹³C NMR (after 8 weeks, 125.77 MHz, C₆D₆): δ 16.5 (d, ¹J_{CP} = 20.7 Hz, CH₃, PMe₃), 26.1 (CH₂, cy C³), 26.2 (CH₂, cy C⁴), 29.7 (broad, CH₂, cy C²), 52.3, 55.4 (py and pz CH₂), 64.4 (CH, cy C¹), 98.3 (CH, pz C⁴), 122.2 (CH, py C³), 124.6 (CH, py C⁵), 137.5 (CH, py C⁴), 149.3 (C, pz C^{3,5}), 150.8 (CH, py C⁶), 158.7 (C, py C²). ¹³C NMR (125.77 MHz, THF-*d*₈): δ 16.7 (d, ¹J_{CP} = 20.4 Hz, CH₃, PMe₃), 26.8 (CH₂, cy C³), 26.9 (CH₂, cy C⁴), 30.5 (broad, CH₂, cy C²), 52.6, 56.1 (py and pz CH₂), 65.2 (CH, cy C¹), 98.4 (CH, pz C⁴), 123.3 (CH, py C⁵), 124.5 (CH, py C³), 124.5 (CH, py C³), 138.3 (CH, py C⁴), 149.8 (C, pz C^{3,5}), 150.7 (CH, py C⁶), 160.3 (C, py C²). ³¹P NMR (202.46 MHz, C₆D₆): δ −51.1 (s). ³¹P NMR (202.46 MHz, THF-*d*₈): δ −50.9 (s). MS (ESI(+)) in CH₃CN): *m/z* (relative intensity) 837.4 (3) [M + H]⁺, 749.3 (10) [L³Cu₂(PMe₃)₂]⁺, 673.2 (55) [L³Cu₂(PMe₃)₂]⁺, 611.3 (71) [L³Cu(PMe₃) + H]⁺, 597.2 (89) [L³Cu]⁺, 535.5 (100) [L³Cu + H]⁺, 215.1 (93) [Cu(PMe₃)₂]⁺.

2. To a solution of L^6H (291 mg, 0.60 mmol) in THF (10 mL) was added a solution of $KOtBu$ (67 mg, 0.60 mmol) in THF (10 mL). After the mixture was stirred for 30 min, the solvent was removed in vacuo. The resulting brownish solid residue was dissolved in propionitrile (10 mL) and a solution of $[Cu(CH_3CN)_4]BF_4$ (376 mg, 1.20 mmol) in propionitrile (10 mL) was added. A deep red solution had formed, which was treated with a solution of $tBuNC$ (100 mg, 1.20 mmol) in acetonitrile (4.8 mL) via a syringe. After this mixture was stirred for 18 h, the solvents were removed in vacuo. The residue was then dried in vacuo for 2 h and extracted with CH_2Cl_2 (10 mL), and the obtained suspension was filtered. The clear solution was stored for 8 days at $-32^\circ C$ to form a small amount of a colorless precipitate that was filtered off. Slow diffusion of diethyl ether (20 mL) into the solution at $+4^\circ C$ over the course of 3 days afforded pale yellow crystals. The yellow solution was decanted; the solid was washed with diethyl ether (20 mL) and finally dried for 12 h in vacuo. **2** was obtained as a beige powder that contained 1.4 equiv of CH_2Cl_2 . Yield: 296 mg (0.30 mmol, 50%). Anal. Calcd for $C_{41}H_{45}N_8Cu_2BF_4 \cdot 1.4CH_2Cl_2$: C, 51.82; H, 4.90; N, 11.40. Found: C, 51.82; H, 4.97; N, 11.63. 1H NMR (500.13 MHz, THF- d_8): δ 1.56 (s, 18 H, $tBuNC$), 3.06 (s, 6 H, CH_3), 4.19 (s, 4 H, CH_2), 6.83–6.85 (m, 2 H, o -Ph), 7.01–7.05 (m, 1 H, p -Ph), 7.17 (t, $^3J_{HH} = 7.7$ Hz, 2 H, m -Ph), 7.50 (t, $^3J_{HH} = 7.9$ Hz, 2 H, quin H^6), 7.72 (d, $^3J_{HH} = 7.9$ Hz, 2 H, quin $H^{5,7}$), 7.83–7.85 (m, 2 H, quin $H^{5,7}$), 7.88–7.91 (m, 2 H, quin H^3), 8.33–8.35 (m, 2 H, quin H^4), 9.23 (dd, $^4J_{HH} = 1.5$ Hz, $^3J_{HH} = 4.5$ Hz, 2 H, quin H^2). ^{13}C NMR (125.77 MHz, THF- d_8): δ 30.5 (CH_3 , $tBuNC$), 47.1 (N- CH_3), 57.3 (C, $tBuNC$), 60.3 (CH_2), 114.2 (C, pz C^4), 124.2 (CH, broad, quin $C^{5,7}$), 124.4 (CH, broad, quin C^3), 125.3 (CH, p -Ph), 126.9 (CH, quin $C^{5,7}$), 127.8 (CH, quin C^6), 128.8 (CH, m -Ph), 129.0 (CH, o -Ph), 130.6 (C, quin C^{4a}), 136.1 (C, i -Ph, $tBuNC$), 138.1 (CH, quin C^4), 143.6 (C, quin C^{8a}), 145.9 (C, pz $C^{3,5}$), 150.9 (C, quin C^8), 152.1 (CH, broad, quin C^2). One signal of a quaternary aromatic carbon atom is not observed but is likely hidden by another resonance in the aromatic region of the spectrum. MS (ESI(+)) in CH_3CN : m/z (relative intensity) 609.0 (27) [L^6Cu_2] $^+$, 483.2 (6) [L^6] $^+$, 453.0 (11) [$L^6Cu_2 - (C_{10}H_9N_2) + H$] $^+$, 389.1 (100) [$L^6Cu - (C_{10}H_9N_2)$] $^+$, 219.1 (69) [$(C_{10}H_8N_2)Cu$] $^+$. IR (KBr): ν_{N-C} 2155 cm^{-1} .

General Procedure for the Preparation of 3–8. A solution of mesitylcopper (including varying amounts of toluene, determined by 1H NMR) in toluene or THF was treated with a solution of the corresponding ligand L^1H – L^6H in toluene or THF at $-78^\circ C$ by means of a cannula. After the mixture was stirred at room temperature overnight, the solvent was concentrated to 5 mL and the reaction mixture was filtered. A 5 mL portion of toluene or THF was added. Oxygen (dried with P_2O_5) was slowly bubbled into the solution via a syringe. Depending on the ligand used, the golden orange to brown solution immediately became dark red to brown. After it was stirred for 2 h, the clear solution was layered with diethyl ether (or pentane for a solution of **6** in diethyl ether, 10 mL) and stored for about 1 week at $-18^\circ C$. The first crystalline crop of the complex was isolated by filtration. In the case of **3** and **7** the filtrate was concentrated to a volume of ca. 2 mL and treated with pentane (20 mL) to give more of the beige precipitate, which was then removed by filtration. The remaining clear solution was again concentrated to a volume of ca. 2 mL, treated with pentane (20 mL), and filtered. The unified solid fractions were washed with pentane (3 \times 5 mL) and dried in vacuo for 14 h.

3. This complex was prepared from a solution of L^1H (164 mg, 0.49 mmol) in THF (10 mL) and a solution of $CuMes \cdot 0.14(toluene)$ (390 mg, 1.99 mmol) in THF (10 mL) as well as oxygen (2.8 mL, 0.12 mmol). An orange powder was obtained. Yield: 278 mg (0.17 mmol, 69%). Anal. Calcd for $C_{74}H_{90}N_{12}OCu_8$: C, 53.16; H, 5.43; N, 10.05. Found: C, 52.90; H, 5.39; N, 9.80. 1H NMR (500.13 MHz, C_6D_6): δ 1.73 (s, 12 H, N- CH_3), 2.20 (s, 12 H, p - CH_3), 2.60 (s, 24 H, o - CH_3), 3.15 (s, 8 H, py CH_2), 3.32 (s, 8 H, pz CH_2), 5.95 (s, 2 H, pz H^4), 6.39 (d, $^3J_{HH} = 7.7$ Hz, 4H, py H^3), 6.74–6.76 (m, 4 H, py H^5), 6.78 (s, 8 H, m -Mes), 6.89 (dt,

Table 5. Crystal Data and Refinement Details for L^3H , **1, and **2****

	L^3H	1	2
formula	$C_{29}H_{40}N_6$	$C_{35}H_{57}N_6 \cdot P_2Cu_2BF_4$	$C_{41}H_{45}N_8 \cdot Cu_2BF_4 \cdot CH_2Cl_2$
M_r	472.67	837.71	948.68
cryst size (mm)	$0.14 \times 0.11 \times 0.10$	$0.25 \times 0.20 \times 0.20$	$0.48 \times 0.29 \times 0.18$
cryst syst	monoclinic	triclinic	triclinic
space group	$P2_1/c$	$P\bar{1}$	$P\bar{1}$
a (Å), α (deg)	11.9534(8), 90	11.157(2), 91.60(3)	13.0195(8), 70.774(5)
b (Å), β (deg)	6.1044(4), 101.041(6)	11.544(2), 97.93(3)	13.2270(8), 75.933(5)
c (Å), γ (deg)	18.5872(15), 90	31.350(6), 92.49(3)	14.2430(8), 72.910(5)
V (Å 3)	1331.17(16)	3993.0(14)	2184.4(2)
Z	2	4	2
ρ_{calcd} ($g\ cm^{-3}$)	1.174	1.393	1.442
$F(000)$	512	1752	976
μ (mm^{-1})	0.072	2.500	1.153
T_{max}/T_{min}		0.6347/0.5738	0.8558/0.6325
hkl range	$\pm 14, \pm 7, -22$ to $+19$	$\pm 12, \pm 13, 0-36$	-14 to $+16, \pm 16, \pm 18$
θ range (deg)	1.74–26.08	1.42–64.79	1.53–26.98
no. of measd rflns	19 477	32 969	40 954
no. of unique rflns (R_{int})	19 477 (0)	11 796 (0.0374)	9463 (0.0808)
no. of data/restraints/params	19 477/1/183	11 798/1206/996	9463/0/540
goodness of fit	1.017	1.044	1.016
$R1$ ($I > 2\sigma(I)$)	0.0481	0.0329	0.0472
w $R2$ (all data)	0.1126	0.0928	0.1206
resid electron	0.290/	0.699/–0.572	0.885/–1.406
density ($e\ \text{\AA}^{-3}$)	–0.149		

$^4J_{HH} = 1.7$ Hz, $^3J_{HH} = 7.6$ Hz, 4 H, py H^4), 9.89 (d, $^3J_{HH} = 4.4$ Hz, 4 H, py H^6). ^{13}C NMR (125.77 MHz, C_6D_6): δ 21.5 (CH_3 , p - CH_3), 29.6 (CH_3 , o - CH_3), 43.1 (CH_3 , N- CH_3), 56.2 (CH_2 , pz CH_2), 61.2 (CH_2 , py CH_2), 97.7 (CH, pz C^4), 122.3 (CH, py C^3), 123.0 (CH, py C^5), 124.4 (CH, m -Mes), 135.5 (C, Mes), 135.8 (CH, py C^4), 137.3 (C, Mes), 147.1 (C, pz $C^{3,5}$, Mes, py C^2), 152.0 (CH, py C^6), 153.4 (C, pz $C^{3,5}$, Mes, py C^2), 157.8 (C, pz $C^{3,5}$, Mes, py C^2). MS (ESI(+)) in THF: m/z (relative intensity) 1222.9 (7) [$L^1Cu_4Mes_3Cu(C_{12}H_{16}N_4)$] $^+$, 1006.9 (5) [$L^1Cu_4Mes_3Cu$] $^+$, 825.0 (18) [$L^1Cu_2Mes_2Cu_2$] $^+$, 643.1 (36) [L^1Cu_3Mes] $^+$, 461.2 (100) [L^1Cu_2] $^+$.

5. This complex was prepared from a solution of L^3H (199 mg, 0.42 mmol) in toluene (10 mL) and a solution of $CuMes \cdot 0.09(toluene)$ (323 mg, 1.69 mmol) in toluene (10 mL) as well as oxygen (2.6 mL, 0.11 mmol). A yellow to beige crystalline solid was obtained directly from layering the reaction solution with diethyl ether. Yield: 194 mg (0.10 mmol, 48%). Anal. Calcd for $C_{94}H_{122}N_{12}OCu_8$: C, 58.06; H, 6.32; N, 8.64. Found: C, 58.07; H, 6.36; N, 8.32. 1H NMR (500.13 MHz, C_6D_6): δ 0.67–0.74, 0.88–0.96 (m, 12 H, cy $H^{2a,4a}$), 1.00–1.08 (m, 8 H, cy H^{3a}), 1.38–1.40 (m, 8 H, cy H^{2e}), 1.47–1.50 (m, 4 H, cy H^{4e}),

Table 6. Crystal Data and Refinement Details for 3, 5, and 6

	3	5	6
formula	1.5C ₇₄ H ₉₀ N ₁₂ OCu ₈ · C ₄ H ₈ O	C ₉₄ H ₁₂₂ N ₁₂ OCu ₈ · 2C ₄ H ₁₀ O·C ₇ H ₈	1.25C ₁₀₆ H ₁₃₀ N ₁₂ OCu ₈ · 5C ₄ H ₁₀ O
M _r	2580.04	2184.80	2991.38
cryst size (mm)	0.20 × 0.10 × 0.10	0.30 × 0.11 × 0.04	0.30 × 0.20 × 0.15
cryst syst	monoclinic	triclinic	tetragonal
space group	C2/c	P $\bar{1}$	I4 ₁ /a
a (Å), α (deg)	64.988(13), 90	17.4933(7), 112.961(3)	42.615(6), 90
b (Å), β (deg)	17.154(3), 100.91(3)	18.5505(7), 93.578(3)	42.615(6), 90
c (Å), γ (deg)	21.229(4), 90	19.8633(7), 111.651(3)	32.935(7), 90
V (Å ³)	23 238(8)	5353.7(3)	59 812(17)
Z	8	2	16
ρ _{calcd.} (g cm ⁻³)	1.475	1.355	1.329
F(000)	10 616	2288	25 160
μ (mm ⁻¹)	2.752	1.611	1.954
T _{max} /T _{min}	0.7704/0.6090	0.8404/0.6501	0.7582/0.5917
hkl range	-32 to +64, ±17, -20 to +19	-22 to +21, ±23, ±25	±33, 0 to 47, 0 to 36
θ range (deg)	2.67–50.43	1.31–26.84	1.70–60.01
no. of measd rflns	49 878	51 169	22 216
no. of unique rflns (R _{int})	11 778 (0.0470)	22 690 (0.0832)	22 216
no. of data/restraints/params	11 778/1992/1598	22 690/11/1153	22 216/2210/1851
goodness of fit	3.206	1.002	1.278
R1 (I > 2σ(I))	0.0916	0.0637	0.0667
wR2 (all data)	0.3082	0.1112	0.2227
resid electron density (e Å ⁻³)	0.878/–0.744	0.699/–0.745	0.922/–0.903

1.53–1.56 (m, 8 H, cy H^{3e}), 1.76–1.82 (m, 4 H, cy H¹), 2.25 (s, 12 H, *p*-CH₃), 2.57 (s, 24 H, *o*-CH₃), 3.44 (broad), 3.54 (2 × s, 16 H, py and pz CH₂), 5.98 (s, 2 H, pz H⁴), 6.38–6.40 (m, 4H, py H³), 6.79 (s, 8 H, *m*-Mes), 6.90–6.95 (m, 8 H, py H^{4,5}), 9.98–9.99 (m, 4 H, py H⁶). ¹³C NMR (125.77 MHz, C₆D₆): δ 21.7 (CH₃, *p*-CH₃), 26.4 (CH₂, cy C³), 26.5 (CH₂, cy C⁴), 28.7 (CH₂, broad, cy C²), 29.6 (CH₃, *o*-CH₃), 51.5, 54.8 (py and pz CH₂), 63.3 (CH, cy C¹), 97.8 (CH, pz C⁴), 121.6 (CH, py C³), 122.7 (CH, py C⁵), 124.7 (CH, *m*-Mes), 135.6 (C, Mes), 135.9 (CH, py C⁴), 137.1 (C, Mes), 148.2 (C, pz C^{3,5}, Mes, py C²), 151.7 (CH, py C⁶), 153.9, 160.0 (C, pz C^{3,5}, Mes, py C²). MS (ESI(+)) in THF: *m/z* (relative intensity) 1818.9 (1) [M – Mes]⁺, 1495.0 (3) [L³Cu₂-Mes₂Cu₃L³]⁺, 1313.2 (9) [L³Cu₂MesCu₂L³]⁺, 1143.0 (2) [L³Cu₂-Mes₂Cu₂MesCu]⁺, 961.2 (56) [L³Cu₂Mes₂Cu₂]⁺, 779.2 (11) [L³Cu₂-MesCu]⁺, 597.4 (26) [L³Cu₂]⁺.

6. This complex was prepared from a solution of L⁴H (236 mg, 0.43 mmol) in toluene (10 mL) and a solution of CuMes·0.09 (toluene) (332 mg, 1.74 mmol) in toluene (10 mL) as well as oxygen (2.7 mL, 0.11 mmol). A yellow to beige crystalline solid was obtained directly from layering a solution of the product in diethyl ether (10 mL) with pentane. Yield: 276 mg (0.13 mmol, 60%). Anal. Calcd for C₁₀₆H₁₃₀N₁₂OCu₈: C, 60.72; H, 6.25; N, 8.02. Found: C, 60.22; H, 6.82; N, 7.79. ¹H NMR (500.13 MHz, C₆D₆): δ ~0.63 (s, broad, 8 H, cy H^{2a}), 0.88–0.93 (m, 4 H, cy H^{4a}), 0.99–1.07 (m, 8 H, cy H^{3a}), 1.37–1.39 (m, 8 H, cy H^{2e}), 1.46–1.48 (m, 4 H, cy H^{4e}), 1.51–1.53 (m, 8 H, cy H^{3e}), 1.80–1.86 (m, 4 H, cy H¹), 2.28 (s, 12 H, *p*-CH₃), 2.60 (s, broad, 24 H, *o*-CH₃), ~3.29 (s, broad, 8 H, py CH₂), 3.74 (s, 8 H, pz CH₂), 6.29–6.31 (m, 4H, py H³), 6.85 (s, 8 H, *m*-Mes), 6.91–6.96 (m, 8 H, py H^{4,5}), 7.09–7.13 (m, 2 H, *p*-Ph), 7.32–7.33 (m, 8 H, *o*-, *m*-Ph), 10.05–10.06 (m, 4 H, py H⁶). ¹³C NMR (125.77 MHz, C₆D₆): δ 21.7 (CH₃, *p*-CH₃), 26.4 (CH₂, cy C³), 26.5 (CH₂, cy C⁴), 29.7 (CH₃, *o*-CH₃), 50.7 (pz CH₂), 54.6 (py CH₂), 63.5 (CH, cy C¹), 115.4 (C, pz C⁴), 121.5 (CH, py C³), 122.7 (CH, py C⁵), 124.6 (CH, *p*-Ph), 124.8

(CH, *m*-Mes), 128.5, 129.4 (CH, *o*-, *m*-Ph), 135.7 (C, *i*-Ph, Mes), 136.0 (CH, py C⁴), 137.2, 137.3 (C, *i*-Ph, Mes), 145.5 (C, pz C^{3,5}, Mes, py C²), 151.8 (CH, broad, py C⁶), ~154.0 (broad), 160.1 (C, pz C^{3,5}, Mes, py C²). The CH₂ resonance signal of cy C² is too broad to be detected. MS (ESI(+)) in THF: *m/z* (relative intensity) 1970.9 (7) [M – Mes]⁺, 1465.2 (17) [L⁴Cu₂MesCu₂L⁴]⁺, 1219.2 (4) [L⁴Cu₂Mes₂Cu₂MesCu]⁺, 1037.2 (49) [L⁴Cu₂Mes₂Cu₂]⁺, 855.2 (12) [L⁴Cu₂MesCu]⁺, 673.4 (36) [L⁴Cu₂]⁺, 421.3 (26) [L⁴Cu – (N(C₆H₁₁)CH₂(C₅H₄N))]⁺, 360.3 (100) [L⁴H – (N(C₆H₁₁)CH₂(C₅H₄N))]⁺, 359.3 (100) [L⁴H – (N(C₆H₁₁)CH₂(C₅H₄N))]⁺.

7. This complex was prepared from a solution of L⁵H (272 mg, 0.48 mmol) in toluene (10 mL) and a solution of CuMes·0.14 (toluene) (374 mg, 1.91 mmol) in toluene (10 mL) as well as oxygen (2.7 mL, 0.11 mmol). A beige powder was obtained. Yield: 394 mg (0.18 mmol, 75%). Anal. Calcd for C₁₀₆H₁₁₀N₁₆OCu₈: C, 59.70; H, 5.20; N, 10.51. Found: C, 59.21; H, 5.24; N, 10.35. ¹H NMR (300.13 MHz, C₆D₆, signals attributed to the labile or noncoordinating pyridyl side groups are denoted with asterisks): δ 2.22 (s, 12 H, *p*-CH₃), 2.72 (s, 24 H, *o*-CH₃), 3.52 (s, 16 H, py CH₂), 3.90 (s, 8 H, pz CH₂), 3.99 (broad, CH₂*), 6.61 (d, ³J_{HH} = 7.7 Hz, 8 H, py H³), 6.67–6.72 (m, 8 H, py H⁵), 6.88 (s, 8 H, *m*-Mes), 6.92 (dt, ⁴J_{HH} = 1.8 Hz, ³J_{HH} = 7.6 Hz, 8 H, py H⁴), 6.96–6.97 (m, 2 H, *p*-Ph), 7.12–7.17 (m, 4 H, *m*-Ph), 7.22–7.25 (m, broad, py*), 7.30–7.33 (m, 4 H, *o*-Ph), 7.41–7.47, 7.84, 8.24–8.26, 9.07 (4 × m, broad, py*), 9.23–9.25 (m, 8 H, py H⁶). ¹³C NMR (75.47 MHz, C₆D₆): δ 21.5 (CH₃, *p*-CH₃), 29.8 (CH₃, *o*-CH₃), 51.2 (pz CH₂), 57.2 (py CH₂), 115.6 (C, pz C⁴), 121.8, 122.0 (py*), 122.4 (CH, py C³), 123.6 (CH, py C³), 124.4 (CH, *p*-Ph), 124.8 (CH, *m*-Mes), ~128.0 (CH, *m*-Ph, overlaid by the benzene signal), 129.2 (CH, *o*-Ph), 135.6 (C, *i*-Ph, Mes), 135.7 (CH, py C⁴), 137.1, 138.2 (C), 144.9 (C, pz C^{3,5}, Mes, py C²), 150.8 (CH, py C⁶), 153.7, 158.0 (C, pz C^{3,5}, Mes, py C²). MS (ESI(+)) in THF: *m/z* (relative intensity) 1319.1 (4) [(L⁵)₂Cu₃]⁺, 1055.0 (18) [L⁵Cu₂Mes₂Cu₂]⁺, 873.1 (16) [L⁵Cu₂MesCu]⁺, 691.3

(57) $[\text{L}^5\text{Cu}_2]^+$, 430.3 (27) $[\text{L}^5\text{Cu} - (\text{N}(\text{CH}_2(\text{C}_5\text{H}_4\text{N}))_2)]^+$, 369.3 (86) $[\text{L}^5\text{H} - (\text{N}(\text{CH}_2(\text{C}_5\text{H}_4\text{N}))_2) + \text{H}]^+$, 368.3 (100) $[\text{L}^5\text{H} - (\text{N}(\text{CH}_2(\text{C}_5\text{H}_4\text{N}))_2)]^+$.

8. This complex was prepared from a solution of L^6H (147 mg, 0.30 mmol) in toluene (10 mL) and a solution of $\text{CuMes} \cdot 0.06(\text{toluene})$ (263 mg, 1.40 mmol) in toluene (10 mL) as well as oxygen (2.0 mL, 0.08 mmol). A precipitate was formed from the stirred reaction mixture that was collected by filtration after cooling for 10 days. This solid was washed with diethyl ether (5×2 mL) and dried in vacuo for 14 h. Yield: 174 mg (0.09 mmol, 60%). Anal. Calcd for $\text{C}_{98}\text{H}_{98}\text{N}_{12}\text{OCu}_8$: C, 59.80; H, 5.02; N, 8.54. Found: C, 59.77; H, 5.48; N, 8.47. ^1H NMR (500.13 MHz, C_6D_6): δ 2.08 (s, 12 H, *p*-CH₃), 2.17 (s, 12 H, *N*-CH₃), 2.52 (s, 24 H, *o*-CH₃), 4.16 (s, 8 H, CH₂), 6.48 (s, 8 H, *m*-Mes), 6.72–6.76 (m, 8 H, quin H³, quin H^{5,7} or *o*-Ph), 6.89–6.92 (m, 4 H, quin H⁶ or *m*-Ph), 6.96–6.97 (m, 4 H, quin H^{5,7} or *o*-Ph), 7.03–7.05, 7.18–7.19 (2 × m, 10 H, quin H, Ph), 7.43 (dd, $^4J_{\text{HH}} = 1.2$ Hz, $^3J_{\text{HH}} = 8.3$ Hz, 4 H, quin H⁴), 9.27–9.28 (m, 4 H, quin H²). ^{13}C NMR (125.77 MHz, C_6D_6): δ 21.5 (CH₃, *p*-CH₃), 29.8 (CH₃, *o*-CH₃), 42.1 (CH₃, *N*-CH₃), 57.3 (CH₂), 115.0 (C, *pz* C⁴), 119.5, 122.0 (CH, quin C³, quin C^{5,7}, or *o*-Ph), 122.8 (CH, quin C^{5,7} or *o*-Ph), 124.6 (CH, *m*-Mes), 124.8 (CH, *p*-Ph), 126.5 (CH, quin C⁶, or *m*-Ph), 128.3, 129.4 (CH, quin C, Ph), 129.8, 134.5 (C), 135.7 (CH, quin C⁴), 136.4, 136.5, 143.1, 145.9 (C), 150.1 (CH, quin C²), 150.2, 154.5 (C). MS (ESI in CH₃CN): *m/z* (relative intensity) 927.1 (16) $[\text{L}^6\text{Cu}_2\text{Mes}_2\text{CuO} + \text{H}]^+$, 847.1 (15) $[\text{L}^6\text{Cu}_2\text{Mes}_2]^+$, 609.2 (95) $[\text{L}^6\text{Cu}_2]^+$, 545.3 (58) $[\text{L}^6\text{Cu} - \text{H}]^+$.

9. The reaction was performed according to the procedure described for 8-(dimethylamino)naphthylcopper(I)^{34a} by using a solution of **4** (109 mg, 0.06 mmol) in toluene (30 mL) and a 0.5 M solution of DMADC in toluene (0.96 mL, 0.48 mmol). Instead of a chromatographic workup, filtration was used to separate the insoluble reaction products. A yellow oil was obtained. ^1H NMR data reveal the formation of **9** and L^2H in a molar ratio of 1.2:1 (expected ratio 2:1). ^1H NMR (500.13 MHz, C_6D_6): δ 2.05 (s, 3 H, *p*-CH₃), 2.33 (s, 6 H, *o*-CH₃), 3.33, 3.41 (2 × s, 6 H, OCH₃), 5.77 (s, 1 H, HC=C), 6.69–6.70 (m, 2 H, *m*-Mes). MS (EI): *m/z* (relative intensity) 262 (2) $[\text{M}]^+$, 247 (3) $[\text{M} - \text{CH}_3]^+$, 231 (16) $[\text{M} - \text{OCH}_3]^+$, 230 (40) $[\text{M} - \text{OCH}_3 - \text{H}]^+$, 203 (40) $[\text{M} - (\text{CO})\text{OCH}_3]^+$, 202 (100) $[\text{M} - (\text{CO})\text{OCH}_3 - \text{H}]^+$, 143 (57) $[\text{M} - \text{Mes}]^+$, 128 (26) $[\text{M} - \text{Mes} - \text{CH}_3]^+$.

X-ray Crystallography. X-ray data for L^3H and **2**, **5**, **7**, and **8** were collected on a STOE IPDS II diffractometer (graphite-monochromated Mo K α radiation, $\lambda = 0.71073$ Å) by use of ω scans at -140 °C (Tables S–7). The structures were solved by direct methods and refined by full-matrix least-squares procedures on F^2 using all reflections with SHELX-97.⁴² Non-hydrogen atoms were refined anisotropically. Hydrogen atoms were placed in calculated positions (riding model) and assigned to an isotropic displacement parameter of 0.08 Å². In the case of L^3H the crystal under investigation was found to be nonmerohedrally twinned (twin law: $-1, 0, 0.25, 0, -1, 0, 0, 1$). An HKLF 5 format file was used for the refinement of the structure. The twin ratio was refined to 0.4535(5)/0.5465(5). Additionally the central pyrazole moiety is disordered about a center of inversion and was refined at half-occupancy. SADI restraints ($d_{\text{C}-\text{C}}$) were used to model the disorder. Parts of the ligand are also disordered in **5** and **7**. For the disordered cyclohexyl moiety in **5** no constraints or restraints were applied (occupancy factors 0.848(8)/0.152(8)), whereas in **7** SADI ($d_{\text{C}-\text{C}/\text{N}}$) and FLAT restraints and EADP (N18A/B) constraints were used to model the disorder of two pyridyl groups (occupancy factors 0.733(13)/0.267(13) and 0.612(17)/0.388(17)). The AFIX 66 instruction was used to model the disorder of one of the phenyl rings bound to the pyrazole moiety in **7** (occupancy factors 0.562(7)/0.438(7)). Furthermore, disordered toluene and diethyl ether molecules are present in **5**, **7**, and **8**. DFIX and SADI restraints and EADP constraints were applied in the case of **5** and **8**. For the solvent molecules in **7** no satisfactory model for the disorder could be found, and for further refinement the contribution of the missing

Table 7. Crystal Data and Refinement Details for **7** and **8**

	7	8
formula	$\text{C}_{106}\text{H}_{110}^-$ $\text{N}_{16}\text{OCu}_8$	$\text{C}_{98}\text{H}_{98}\text{N}_{12}\text{OCu}_8 \cdot$ $\text{C}_4\text{H}_{10}\text{O} \cdot 0.5 \text{C}_7\text{H}_8$
M_r	2132.48	2088.47
cryst size (mm)	0.29 × 0.19 × 0.16	0.36 × 0.24 × 0.14
cryst syst	monoclinic	triclinic
space group	$C2/c$	$P\bar{1}$
a (Å), α (deg)	25.1096(6), 90	15.6032(7), 67.364(3)
b (Å), β (deg)	50.2683(11), 91.799(2)	18.6504(7), 86.560(3)
c (Å), γ (deg)	18.3179(5), 90	19.8654(8), 66.561(3)
V (Å ³)	23109.8(10)	4865.7(3)
Z	8	2
ρ_{calcd} (g cm ⁻³)	1.226	1.425
$F(000)$	8784	2154
μ (mm ⁻¹)	1.491	1.768
$T_{\text{max}}/T_{\text{min}}$	0.8216/0.6789	0.7951/0.5641
hkl range	−30 to +27, ±61, ±22	±18, ±21, −22 to +23
θ range (deg)	1.38–26.00	1.43–24.79
no. of measd rflns	120 104	104 897
no. of unique rflns (R_{int})	22 614 (0.0624)	16 639 (0.1150)
no. of data/ restraints/params	22 614/128/1152	16 639/16/1140
goodness of fit	1.019	1.008
$R1$ ($I > 2\sigma(I)$)	0.0589	0.0563
w $R2$ (all data)	0.1572	0.1602
resid electron density (e Å ⁻³)	0.983/−0.802	1.679/−0.555

solvent molecules (4734.3 Å³, electron count 937) was subtracted from the reflection data by the SQUEEZE⁴³ routine of the PLATON⁴⁴ program. Face-indexed absorption corrections for **2**, **5**, **7**, and **8** were performed numerically with the program X-RED.⁴⁵

X-ray data for **1**, **3**, and **6** were collected on a Bruker three-circle diffractometer with a SMART 6000 detector and Cu K α radiation ($\lambda = 1.54178$ Å) at -178 °C. The crystal of compound **1** that was used was a nonmerohedral twin, and two domains (0.529/0.471) could be identified with the program CELL_NOW.⁴⁶ Both domains were used for integration. Absorption and intensity data were corrected with the TWINABS program.⁴⁷ The structure was solved using direct methods and refined by full-matrix least-squares procedures against F^2 using all reflections with SHELX-97.⁴² Non-hydrogen atoms were refined anisotropically, and hydrogen atoms were placed in calculated positions using the riding model. In the asymmetric unit two independent complex molecules and two BF_4^- counterions could be refined. Since all BF_4^- counterion molecules are disordered through a symmetry center, SADI restraints were used to equal bond lengths and angles.

In the case of compound **3** a multidomain split crystal was used, but single domains could be identified. The structure was solved using direct methods and refined by full-matrix least-squares procedures against F^2 using all reflections with SHELX-97.⁴² Two possible space groups ($C2/c$ and Cc) could be found that gave equal results and disorder. Thus, the higher symmetric space group $C2/c$ was chosen. Non-hydrogen atoms were refined anisotropically, and hydrogen atoms were placed in calculated positions using the riding model. In the asymmetric unit two independent complex molecules and one disordered THF solvent molecule could be refined. Because of complex and solvent disorder,

FLAT, DFIX, and DANG as well as SIMU and DELU restraints were used.

Absorption and intensity data of compound **6** were corrected with the SADABS program. The structure was solved in the tetragonal space group $I4_1/a$ using direct methods and refined by full-matrix least-squares procedures against F^2 . Non-hydrogen atoms were refined anisotropically, and hydrogen atoms were placed in calculated positions using the riding model. In the asymmetric unit two independent complex molecules and five partially disordered ether molecules could be refined. Since the cyclohexyl groups in the complex as well as the solvent molecules are disordered, SADI, DFIX, DANG, SIMU, and DELU restraints were used.

■ ASSOCIATED CONTENT

S Supporting Information. CIF files giving crystallographic data for **L**³**H** and **1–8**, figures giving molecule plots with anisotropic displacement factors, and tables giving selected interatomic distances and angles of **5–8** as well as of all independent molecules in the asymmetric unit of the crystal structures of **3** and **6**. This material is available free of charge via the Internet at <http://pubs.acs.org>.

■ AUTHOR INFORMATION

Corresponding Author

*M.S.: tel, +1 979 845 5978; fax, +1 979 845 5629; e-mail, mstollenz@mail.chem.tamu.edu. F.M.: tel, +49 551 393012; fax, +49 551 393063; e-mail, franc.meyer@chemie.uni-goettingen.de.

Present Addresses

[†]Department of Chemistry, Texas A&M University, 580 Ross Street, P.O. Box 30012, College Station, Texas 77842–3012.

■ ACKNOWLEDGMENT

We thank Prof. G. M. Sheldrick for providing X-ray data collection facilities, Dr. Michael John (Institute for Inorganic Chemistry at the University of Göttingen) for helpful discussions, Dr. Holm Frauendorf (Institute for Organic and Biomolecular Chemistry at the University of Göttingen) for measuring HR mass spectra, and the Fonds der Chemischen Industrie for financial support.

■ REFERENCES

- (1) Krause, N. *Modern Organocopper Chemistry*; Wiley-VCH: Weinheim, Germany, 2002.
- (2) General reviews: (a) Kitajima, N.; Moro-oka, Y. *Chem. Rev.* **1994**, *94*, 737–757. (b) van der Vlugt, J. I.; Meyer, F. *Top. Organomet. Chem.* **2007**, *22*, 191–240.
- (3) Oxidative alkyne coupling: Siemsen, P.; Livingston, R. C.; Diederich, F. *Angew. Chem.* **2000**, *112*, 2740–2767; *Angew. Chem., Int. Ed.* **2000**, *39*, 2632–2657.
- (4) Oxidative aryl coupling: (a) Camus, A.; Marsich, N. *J. Organomet. Chem.* **1972**, *46*, 385–394. (b) Kauffmann, T. *Angew. Chem.* **1974**, *86*, 321–335; *Angew. Chem., Int. Ed. Engl.* **1974**, *13*, 291–305. (c) van Koten, G.; Jastrzebski, J. T. B. H.; Noltes, J. G. *J. Org. Chem.* **1977**, *42*, 2047–2053. (d) Lipshutz, B. H.; Siegmann, K.; Garcia, E. *Tetrahedron* **1992**, *48*, 2579–2588. (e) Lipshutz, B. H.; Siegmann, K.; Garcia, E.; Kayser, F. *J. Am. Chem. Soc.* **1993**, *115*, 9276–9282. (f) Noji, M.; Nakajima, M.; Koga, K. *Tetrahedron Lett.* **1994**, 7983–7984. (g) Nakajima, M.; Miyoshi, I.; Kanayama, K.; Hashimoto, S.-i.; Noji, M.; Koga, K. *J. Org. Chem.* **1999**, *64*, 2264–2271. (h) Surry, D. S.; Spring,

D. R. *Chem. Soc. Rev.* **2006**, *35*, 218–225. (i) Temma, T.; Hatano, B.; Habauze, S. *Tetrahedron* **2006**, *62*, 8559–8563.

(5) See for example: (a) Rossiter, B. E.; Swingle, N. M. *Chem. Rev.* **1992**, *92*, 771–806. (b) Nakajima, R.; Delas, C.; Takayama, Y.; Sato, F. *Angew. Chem.* **2002**, *114*, 3149–3151; *Angew. Chem., Int. Ed.* **2002**, *41*, 3023–3025. (c) Woodward, S. *Angew. Chem.* **2005**, *117*, 5696–5698; *Angew. Chem., Int. Ed.* **2005**, *44*, 5560–5562. (d) López, F.; Minnaard, A. J.; Feringa, B. L. *Acc. Chem. Res.* **2007**, *40*, 179–188. (e) Dubbaka, S. R.; Kienle, M.; Mayr, H.; Knochel, P. *Angew. Chem.* **2007**, *119*, 9251–9255; *Angew. Chem., Int. Ed.* **2007**, *46*, 9093–9096. (f) Alexakis, A.; Bäckvall, J. E.; Krause, N.; Pàmies, O.; Diéguez, M. *Chem. Rev.* **2008**, *108*, 2796–2823.

(6) (a) Tsuda, T.; Yazawa, T.; Watanabe, K.; Fujii, T.; Saegusa, T. *J. Org. Chem.* **1981**, *46*, 192–194. (b) Gambarotta, S.; Floriani, C.; Chiesi-Villa, A.; Guastini, C. *J. Chem. Soc., Chem Commun.* **1983**, 1156–1158. (c) Meyer, E. M.; Gambarotta, S.; Floriani, C.; Chiesi-Villa, A.; Guastini, C. *Organometallics* **1989**, *8*, 1067–1079. (d) Eriksson, H.; Håkansson, M. *Organometallics* **1997**, *16*, 4243–4244.

(7) Leoni, P.; Pasquali, M.; Ghilardi, C. A. *J. Chem. Soc., Chem. Commun.* **1983**, 240–241.

(8) (a) Knotter, D. M.; Smeets, W. J. J.; Spek, A. L.; van Koten, G. *J. Am. Chem. Soc.* **1990**, *112*, 5895–5896. (b) Knotter, D. M.; Grove, D. M.; Smeets, W. J. J.; Spek, A. L.; van Koten, G. *J. Am. Chem. Soc.* **1992**, *114*, 3400–3410. (c) Janssen, M. D.; Donkervoort, J. G.; van Berlekom, S. B.; Spek, A. L.; Grove, D. M.; van Koten, G. *Inorg. Chem.* **1996**, *35*, 4752–4763.

(9) (a) Davies, R. P.; Hornauer, S.; White, A. J. P. *Chem. Commun.* **2007**, 304–306. (b) Davies, R. P.; Hornauer, S.; Hitchcock, P. B. *Angew. Chem.* **2007**, *119*, 5283–5286; *Angew. Chem., Int. Ed.* **2007**, *46*, 5191–5194. (c) Bomparola, R.; Davies, R. P.; Hornauer, S.; White, A. J. P. *Angew. Chem.* **2008**, *120*, 5896–5899; *Angew. Chem., Int. Ed.* **2008**, *47*, 5812–5815. (d) Bomparola, R.; Davies, R. P.; Hornauer, S.; White, A. J. P. *Dalton Trans.* **2009**, 1104–1106.

(10) Håkansson, M.; Örtendahl, M.; Jagner, S.; Sigalas, M. P.; Eisenstein, O. *Inorg. Chem.* **1993**, *32*, 2018–2024.

(11) Stollenz, M.; Grosse, C.; Meyer, F. *Chem. Commun.* **2008**, 1744–1746.

(12) (a) Garilova, A. L.; Bosnich, B. *Chem. Rev.* **2004**, *104*, 349–383. (b) Klingele, J.; Dechert, S.; Meyer, F. *Coord. Chem. Rev.* **2009**, *253*, 2698–2741.

(13) (a) Meyer, F.; Pritzkow, H. *Angew. Chem.* **2000**, *112*, 2199–2202; *Angew. Chem., Int. Ed.* **2000**, *39*, 2112–2115. (b) Ackermann, J.; Meyer, F.; Kaifer, E.; Pritzkow, H. *Chem. Eur. J.* **2002**, *8*, 247–258. (c) Prokofieva, A.; Prikhod'ko, A. I.; Enyedy, E. A.; Farkas, E.; Maringgele, W.; Demeshko, S.; Dechert, S.; Meyer, F. *Inorg. Chem.* **2007**, *46*, 4298–4307. (d) Ackermann, J.; Buchler, S.; Meyer, F. *C. R. Chim.* **2007**, *10*, 421–432. (e) Prokofieva, A.; Prikhod'ko, A. I.; Dechert, S.; Meyer, F. *Chem. Commun.* **2008**, 1005–1007. (f) Prokofieva, A.; Dechert, S.; Grosse, C.; Sheldrick, G. M.; Meyer, F. *Chem. Eur. J.* **2009**, *15*, 4994–4997.

(14) (a) Dias, H. V. R.; Diyabalanage, H. V. K.; Rawashdeh-Omary, M. A.; Franzman, M. A.; Omary, M. A. *J. Am. Chem. Soc.* **2003**, *125*, 12072–12073. (b) Dias, H. V. R.; Diyabalanage, H. V. K.; Eldabaja, M. G.; Elbjairami, O.; Rawashdeh-Omary, M. A.; Omary, M. A. *J. Am. Chem. Soc.* **2005**, *127*, 7489–7501. (c) Omary, M. A.; Rawashdeh-Omary, M. A.; Gonser, M. W. A.; Elbjairami, O.; Grimes, T.; Cundari, T. R.; Diyabalanage, H. V. K.; Gamage, C. S. P.; Dias, H. V. R. *Inorg. Chem.* **2005**, *44*, 8200–8210.

(15) Stollenz, M.; John, M.; Gehring, H.; Dechert, S.; Grosse, C.; Meyer, F. *Inorg. Chem.* **2009**, *48*, 10049–10059.

(16) Scheele, U. J.; Georgiou, M.; John, M.; Dechert, S.; Meyer, F. *Organometallics* **2008**, *27*, 5146–5151.

(17) (a) Ardizzoia, G. A.; Beccalli, E. M.; La Monica, G.; Masciocchi, N.; Moret, M. *Inorg. Chem.* **1992**, *31*, 2706–2711. (b) Ardizzoia, G. A.; Cenini, S.; La Monica, G.; Masciocchi, N.; Moret, M. *Inorg. Chem.* **1994**, *33*, 1458–1463. (c) Singh, K.; Long, J. R.; Stavropoulos, P. *Inorg. Chem.* **1998**, *37*, 1073–1079. (d) Ardizzoia, G. A.; Cenini, S.; La Monica, G.; Masciocchi, N.; Maspero, A.; Moret, M. *Inorg. Chem.* **1998**, *37*, 4284–4292.

- (18) Schenck, T. G.; Downes, J. M.; Milne, C. R. C.; Mackenzie, P. B.; Boucher, H.; Whelan, J.; Bosnich, B. *Inorg. Chem.* **1985**, *24*, 2334–2337.
- (19) Sachse, A.; Penkova, L.; Noël, G.; Dechert, S.; Varzatskii, O. A.; Fritsky, I. O.; Meyer, F. *Synthesis* **2008**, *5*, 800–806.
- (20) (a) Foces-Foces, C.; Alkorta, I.; Elguero, J. *Acta Crystallogr.* **2000**, *B56*, 1018–1028. (b) Röder, J. C.; Meyer, F.; Pritzkow, H. *Organometallics* **2001**, *20*, 811–817.
- (21) (a) Raptis, R. G.; Staples, R. J.; King, C.; Fackler, J. P., Jr. *Acta Crystallogr.* **1993**, *C49*, 1716–1719. (b) Goddard, R.; Claramunt, R. M.; Escolástico, C.; Elguero, J. *New J. Chem.* **1999**, 237–240.
- (22) Guerrero, A. M.; Jalón, F. A.; Manzano, B. R.; Claramunt, R. M.; Santa María, M. D.; Escolástico, C.; Elguero, J.; Ana M. Rodríguez, A. M.; Maestro, M. A.; Mahía, J. *Eur. J. Inorg. Chem.* **2002**, 3178–3189.
- (23) Müller, H.; Bauer-Siebenlist, B.; Csapo, E.; Dechert, S.; Farkas, E.; Meyer, F. *Inorg. Chem.* **2008**, *47*, 5278–5292.
- (24) These distances were calculated with the program DIAMOND 3.2e by defining a plane of the five constituent atoms of the pyrazolate heterocycle.
- (25) If the two coordination polyhedra were ideally tetrahedral, the X-ray molecular structure would display the meso form *R,S* of **1**, whereas the corresponding chiral *R,R* and *S,S* isomers are found in **2** (vide infra). Our approach in terms of describing the stereochemistry takes the considerable deviation from tetrahedral symmetry into account, which is observed at the Cu^I centers of **1–8**.
- (26) Bondi, A. J. *Phys. Chem.* **1964**, *68*, 441–451.
- (27) Repetitive experiments reveal often a larger content of mesitylene than is expected, which is attributed to the competing reaction with water. We have previously observed that **3–8** are also formed in small amounts by storing reaction mixtures of L¹H–L⁶H and mesitylcopper (ratio 1:4) under an argon atmosphere, very likely by small traces of water adhering on the surface of the Schlenk flasks. Mesitylene is then supposed to be the only side product from this reaction.
- (28) (a) Lappert, M. F.; Pearce, R. *J. Chem. Soc., Chem. Commun.* **1973**, 24–25. (b) Jarvis, J. A. J.; Kilbourn, B. T.; Pearce, R.; Lappert, M. F. *J. Chem. Soc., Chem. Commun.* **1973**, 475–476.
- (29) The τ value, defined by $\tau = (\beta - \alpha)/60^\circ$, allows an accurate estimation for distinguishing between trigonal-bipyramidal and square-pyramidal coordination in pentacoordinated complexes {L₅}M. α and β represent the largest angles L–M–L' ($\alpha < \beta \leq 180^\circ$). A τ value equal to zero indicates an ideally square-pyramidal coordination sphere, whereas $\tau = 1$ is related to an ideal trigonal bipyramid: Addison, A. W.; Rao, T. N.; Reedijk, J.; van Rijn, J.; Verschoor, G. C. *J. Chem. Soc., Dalton Trans.* **1984**, 1349–1356.
- (30) (a) Guy, J. T., Jr.; Cooper, J. C.; Gilardi, R. D.; Flippen-Anderson, J. L.; George, C. F., Jr. *Inorg. Chem.* **1988**, *27*, 635–638. (b) Keij, F. S.; Haasnoot, J. G.; Oosterling, A. J.; Reedijk, J.; O'Connor, C. J.; Zhang, J. H. *Inorg. Chim. Acta* **1991**, *181*, 185–193. (c) Skorda, K.; Stamatatos, T. C.; Vafiadis, A. P.; Lithoxidou, A. T.; Terzis, A.; Perlepes, S. P.; Mrozinski, J.; Raptopoulou, C. P.; Plakatouras, J. C.; Bakalbassis, E. G. *Inorg. Chim. Acta* **2005**, *358*, 565–582.
- (31) (a) Teipel, S.; Griesar, K.; Haase, W.; Krebs, B. *Inorg. Chem.* **1994**, *33*, 456–464. (b) Reim, J.; Griesar, K.; Haase, W.; Krebs, B. *J. Chem. Soc., Dalton Trans.* **1995**, 2649–2656.
- (32) (a) Gröger, G.; Olbrich, F.; Weiss, E.; Behrens, U. *J. Organomet. Chem.* **1996**, *514*, 81–86. (b) Olbrich, F.; Gröger, G.; Behrens, U. *Z. Kristallogr.* **1999**, *214*, 195–200.
- (33) Restori, R.; Schwarzenbach, D. *Acta Crystallogr.* **1986**, *B42*, 201–208.
- (34) (a) Wehman, E.; van Koten, G.; Knotter, M.; Spelten, H.; Heijdenrijk, D.; Mak, A. N. S.; Stam, C. H. *J. Organomet. Chem.* **1987**, *325*, 293–309. (b) Janssen, M. D.; Corsten, M. A.; Spek, A. L.; Grove, D. M.; van Koten, G. *Organometallics* **1996**, *15*, 2810–2820.
- (35) (a) Edwards, P. G.; Gellert, R. W.; Marks, M. W.; Bau, R. *J. Am. Chem. Soc.* **1982**, *104*, 2072–2073. (b) He, X.; Ruhlandt-Senge, K.; Power, P. P.; Bertz, S. H. *J. Am. Chem. Soc.* **1994**, *116*, 6963–6964.
- (36) Waibel, M.; Kraus, F.; Scharfe, S.; Wahl, B.; Fässler, T. F. *Angew. Chem.* **2010**, *122*, 6761–6765; *Angew. Chem., Int. Ed.* **2010**, *49*, 6611–6615.
- (37) Becker, H. G. O.; Berger, W.; Domschke, G.; Fanghänel, E.; Faust, J.; Fischer, M.; Gentz, F.; Gewalt, K.; Gluch, R.; Mayer, R.; Müller, K.; Pavel, D.; Schmidt, H.; Schollberg, K.; Schwetlick, K.; Seiler, E.; Zeppenfeld, G. *Organikum*, 19th ed.; Johann Ambrosius Barth: Leipzig, Berlin, Heidelberg, Germany, 1993.
- (38) Heckel, E. (Deutsche Gold- und Silberscheideanstalt) Ger. Offen. 1,230,025 (Cl.C 07c,f), 1966; *Chem. Abstr.* **1967**, *66*, 46487e.
- (39) Zára-Kaczián, E.; Deák, G.; György, L. *Acta Chim. Hung.* **1989**, *126*, 441–454.
- (40) Incarvito, C.; Lam, M.; Rhatigan, B.; Rheingold, A. L.; Qin, J.; Gavrilova, A. L.; Bosnich, B. *Dalton Trans.* **2001**, 3478–3488.
- (41) The synthesis of L¹H was previously described in: Bauer-Siebenlist, B. Dissertation, University of Göttingen, Göttingen, Germany, 2004.
- (42) Sheldrick, G. M. *Acta Crystallogr.* **2008**, *A64*, 112–122.
- (43) van der Sluis, P.; Spek, A. L. *Acta Crystallogr.* **1990**, *A46*, 194–201.
- (44) (a) Spek, A. L. *Acta Crystallogr.* **1990**, *A46*, C34. (b) Spek, A. L. *PLATON: A Multipurpose Crystallographic Tool*; Utrecht University, Utrecht, The Netherlands, 2006.
- (45) *X-RED*; STOE & CIE GmbH, Darmstadt, Germany, 2002.
- (46) Sheldrick, G. M. *CELL_NOW*; University of Göttingen, Göttingen, Germany, 2005.
- (47) Sheldrick, G. M. *TWINABS: Program for Performing Absorption Corrections to X-ray Diffraction Patterns Collected from Non-Merohedrally Twinned and Multiple Crystals*; University of Göttingen, Göttingen, Germany, 2002.